Applications of Laser Terrain Mapping in Central Texas for Managing Karst Aquifers and Land Use

Final Report
by

Edward W. Collins, Thomas A. Tremblay, Roberto Gutierrez, Jay A. Raney,
Jennifer Rawlings, Adrien Lindley, and Susan D. Hovorka

prepared for

California Institute of Technology, Jet Propulsion Laboratory
under Contract 1247072 for the NASA-AASG Program

Bureau of Economic Geology
Scott W. Tinker, Director
John A. and Katherine G. Jackson School of Geosciences
The University of Texas at Austin
Austin, Texas 78713-8924

October 2003

Applications of Laser Terrain Mapping in Central Texas for Managing Karst Aquifers and Land Use

Final Report
by

Edward W. Collins, Thomas A. Tremblay, Roberto Gutierrez, Jay A. Raney,
Jennifer Rawlings, Adrien Lindley, and Susan D. Hovorka

prepared for

California Institute of Technology, Jet Propulsion Laboratory
under Contract 1247072 for the NASA-AASG Program

Bureau of Economic Geology
Scott W. Tinker, Director
John A. and Katherine G. Jackson School of Geosciences
The University of Texas at Austin
Austin, Texas 78713-8924

October 2003

CONTENTS

Figures

INTRODUCTION

This investigation illustrates the effectiveness of using airborne laser terrain mapping (ALTM) data, also referred to as lidar data, with QUICKBIRD satellite imagery for mapping applications related to managing karst limestone aquifers and land use in Central Texas. Test-case studies conducted within the south Austin, Texas, area (fig. 1) illustrate the usefulness of lidar data, used alone and in combination with other imagery, for mapping karst-related recharge features, areas prone to slope failure, terraces of flood-prone streams, and faults in hilly limestone terrain.

The south Austin urban and suburban area is an ideal study area to test the applicability of ALTM for geologic mapping. The study area contains developed and undeveloped areas, the region is undergoing rapid urban growth, and the region's geology has a major impact on managing and planning water resources, land use, and construction (Woodruff, 1975; Garner and Young, 1976; Woodruff and Collins, 2001). Geologic maps and knowledge of geologic attributes, such as karst features, faults, and the physical properties of lithologic units and their related soils, are required for managing water-resource, land-use, and construction issues. For example, Cretaceous bedrock of the region includes the prolific Edwards limestone aquifer and its recharge zone. Identification of recharge features such as dolines is required for us to understand groundwater recharge, flow, and quality and for the permitting of many construction projects.

Austin's geology also includes an approximately 140-ft-thick stratigraphic interval composed of Cretaceous Del Rio clay, Buda limestone, and Eagle Ford clay, shale, marl, and bentonite. Clay-rich Del Rio and Eagle Ford strata and their soils exhibit relatively poor slope stability and foundation strength, and the clays have expansive properties that cause swelling when wet and shrinking when dry. Mapping of the higher slope areas that may be prone to slope failure within these strata is important for planning construction projects and maintaining roadways.

The Austin area is also dissected by the Colorado River and its numerous tributaries, and terraces of the larger streams cover a substantial part of Austin's urban-growth corridor. Detailed maps illustrating geologic units that include multiple terraces associated with streams can provide basic information that is useful for land-use planning and suburban development. Maps that accurately depict fault locations are also crucial to professionals managing the area's water resources and land use. Faults of the Balcones Fault Zone are the major controls on the study area's structural framework, including the Edwards aquifer and recharge zone.

This report describes the study results of four test-case topics: (1) mapping of dolines within dry-streambed and upland settings within the Edwards limestone and dolomitic limestone, the primary host unit for the prolific Edwards aquifer; (2) mapping of areas of greater slopes within the Upper Cretaceous Del Rio-Buda-Eagle Ford strata outcrop belt, a clay-rich stratigraphic sequence that is prone to slope failure and foundation problems and is cut by numerous smaller displacement faults; (3) mapping of stream terraces of Onion Creek, a major flood-prone stream dissecting the south Austin region; and (4) mapping of fault strands of the Balcones Fault Zone within hilly limestone terrain.

Lidar data, collected from an ALTM survey, allow for relatively quick, detailed interpretation of closed topographic depressions having widths between about 5 and 30 ft in the Edwards Limestone. The ability to identify these relatively small-scale, closed topographic depressions using remote-sensing methods, as a precursor to field verification and doline mapping in the field, is a

great aid to mapping this type of important recharge feature. Analysis of ATLM data, with the help of high-resolution satellite imagery such as QUICKBIRD and geologic map data, allows for rapid mapping of areas containing relatively steeper slopes within clay-rich strata that are prone to slope failure and foundation problems. Mapping of steeper-slope areas within strata prone to slope failure is useful for planning construction projects, as well as maintaining existing cultural features such as roadways. ATLM data, with the help of high-resolution imagery, facilitate detailed mapping of stream terraces. Acquiring accurate elevation data in order to subdivide stream terraces along potential flood-prone areas within expanding suburban settings may aid suburban planning and land use. Analysis of ATLM data is useful for recognizing local topographic expressions that may reflect faults within Central Texas limestone terrain. Study of ATLM data in local areas may improve existing fault maps or may be a useful aid for new mapping.

METHODS

Data used for this study include ALTM data (also referred to as lidar data in this report), a digital geologic-map data set (Tremblay and Andrews, 1997) of the *Geologic Map of the Austin Area, Texas* (Garner and others, 1976), digital data sets of identified karst features [City of Austin Karst Data Base (Nico Houwert, personal communication, 2003) and Central Texas Geological Assessment database (Jennifer Rawlings and Adrien Lindley, personal communication, 2003)], high-resolution QUICKBIRD satellite imagery (resolution of about 8 ft), and pan-sharpened QUICKBIRD satellite imagery (resolution of about 2 ft). Selected aerial photography was used for some areas that were not within available QUICKBIRD coverage. Lower-resolution, remotely sensed satellite data, such as Landsat imagery, were determined not to meet the high-resolution needs required for this project's study topics. About 100 square miles of ALTM data have been collected for the Austin region. The south Austin data set used for this study was collected during spring 2002. The ALTM surveys are conducted in collaboration with The University of Texas Center for Space Research (CSR). Algorithms developed by CSR for enhanced characterization (vegetation removal) have been applied to most of the Austin lidar data. CSR also provided the high-resolution QUICKBIRD imagery for this study.

Ground-elevation, geologic, and imagery data sets were studied in an Arcview geographic information system. Specific study techniques varied for the different test-case topics, although in general the lidar data were used to construct detailed elevation maps that were used with geologic and imagery data sets to test mapping applications.

GEOLOGIC SETTING

The south Austin study area lies within the Cretaceous outcrop belt that generally trends parallel to the arcuate structural grain of the Miocene-age Balcones Fault Zone that traverses the area (fig. 1). The regional Balcones Escarpment, with topographic relief as great as 300 ft in Austin, is a fault-line scarp of the Balcones Fault Zone (Hill, 1900). In Austin the escarpment trends northerly and separates hilly, dissected Edwards Plateau terrain to the west from the rolling Blackland Prairies terrain to the east. Major normal faults generally strike northward or northeastward and dip between 40° and 80° (Garner and Young, 1976; Collins and Woodruff,

2001). Faults dip both eastward and westward; however, the composite structural relief is down-to-the-east between 1,100 and 1,600 ft. The largest fault has a throw exceeding 650 ft, although most of the faults exhibit throws between a few feet and 100 ft.

Strata in Austin consist mostly of Cretaceous limestone, dolomitic limestone, marl, and shale that represent more than 2,000 ft of shelf and shelf-margin deposition (fig. 2). East of Austin are Paleocene and Eocene marine, deltaic, and fluvial deposits. Terrace alluvium covers bedrock strata along the Colorado River, which flows southeastward through Austin, and its tributaries.

Cretaceous strata include the limestone and dolomitic limestone that compose the prolific Edwards aquifer and its recharge zone. This karstic aquifer is a major water supply for Central Texas. Karst voids within the aquifer strata allow for rapid recharge and transmission of groundwater through the cavities. The aquifer strata also provide habitat for various endangered species. Karst voids in the vadose zone locally provide habitat for a number of arthropods designated as endangered. Also in Austin, one spring system of the aquifer provides habitat for the Barton Springs salamander, also designated as endangered.

MAPPING SURFACE KARST

ALTM data can be used to identify and map closed topographic depressions within karst strata that may be dolines. These data greatly aid ground-based investigations for verifying significant dolines by providing relatively quick, remotely sensed interpretations of subtle features across large or site-specific areas of sometimes rugged terrain.

Figure 3 illustrates the locations of test-case study sites within two settings in the recharge zone of the Edwards aquifer: (1) a dry creek bed of a major perennial creek, Barton Creek, and (2) uplands terrain. Study sites along Barton Creek focused on known sinkholes that have been identified during ground-based studies (figs. 3 through 6). Detailed elevation-contour maps constructed using ALTM data at all of these creek study sites illustrate topographic depressions, with closed contours at the areas where sinkholes had been mapped during previous ground-based studies (City of Austin Karst Data Base and David Johns, personal communication, 2001). Contour intervals of 2 and 3 ft highlight the subtle topographic low areas of known sinkholes, as well as the irregular topography of the creek bed, including some closed topographic contours (depressions) that are not dolines. Ground-based studies are required for verifying dolines, although ALTM data can bolster ground-based studies by speeding up identification of areas to field check.

Study of ALTM data within the uplands terrain of the Edwards aquifer recharge zone included evaluation of parts of the recharge zone in areas where recharge features had been identified. Because much of the area has been urbanized, cultural features such as roads and buildings prevented adequate analysis. As a result, this remote-sensing technique had trouble in identifying small, subtle features across much of the south Austin urban and suburban area where ALTM data are available. However, lidar-based data of three study sites (fig. 3, sites 7, 8, 9) of known sinkholes within local, undeveloped areas that underwent previous ground-based studies (digital data sets of identified karst features mentioned in the Methods section) are presented (figs. 7 through 12). Additionally, lidar-based data of an undeveloped area that has not undergone a ground-based study to identify karst features is presented (fig. 3, site 10, figs. 13, 14). Figures 8, 10, and 12 illustrate detailed ground-elevation contour maps constructed with the help of ALTM data of areas where

sinkholes and caves were mapped during previous studies. Ground-elevation contour maps of the ALTM data illustrate a number of subtle closed topographic depressions covering areas that are between 5 and 30 ft wide. Not all of the previously mapped karst features precisely correlate with closed topographic depressions mapped using lidar data. This fact suggests that some sinkholes may not have enough topographic expression to be identified or possibly that there are not enough lidar data points to identify the smallest, subtlest features. Ground-based studies are required in order to determine how many of the closed topographic depressions mapped using ALTM techniques are karst-related features. However, lidar data can provide detailed maps of remotely sensed closed topographic depressions to support ground-based mapping of dolines. Figures 13 and 14 illustrate another study-site example of a ground-elevation contour map of a site within the Edwards aquifer recharge zone and several remotely mapped closed topographic depressions on a high-resolution satellite image. This example at study site 10 demonstrates that closed topographic features can be identified from lidar data and studied using high-resolution satellite imagery. Identification of the relatively small scaled closed topographic depressions in conjunction with detailed imagery aids ground-based mapping of karst features because specific features can be identified for ground studies.

MAPPING AREAS PRONE TO SLOPE FAILURE

Analysis and comparison of ATLM data, high-resolution imagery and standard geologic map data, allow for the mapping of areas containing relatively high slopes within clay-rich strata that are prone to slope failure and foundation problems. In the Austin study area construction-related concerns of the approximately 140-ft-thick strata interval composed of Cretaceous Del Rio clay, Buda limestone, and Eagle Ford clay, shale, marl, and bentonite have existed for a number of years (Woodruff, 1975; Garner and Young, 1976; Woodruff and Collins, 2001). Construction within clay-rich Del Rio and Eagle Ford deposits requires construction designs and techniques that are much different from those applied in nearby Cretaceous limestone and chalk. Clay-rich Del Rio and Eagle Ford strata and their soils exhibit relatively poor slope stability and foundation strength, and the clays have expansive properties that cause swelling when wet and shrinking when dry. Buda limestone that caps slopes of Del Rio clay can sometimes be unstable because of the poor slope stability of the Del Rio clay. Mapping the higher slope areas within these strata prone to slope failure is useful for planning construction projects, as well as maintaining existing cultural features such as roads.

ALTM data can be analyzed to identify areas having different slope ranges within the Del Rio-Buda-Eagle Ford deposits. Figures 15, 16, and 17 illustrate geologic setting, examples of slope maps and satellite imagery of study site 11. Maps displaying different slope ranges can be generated relatively easily within Arcview. Higher slope areas, shown in figures 16 and 17, may be more prone to slope failure. High-resolution imagery, such as the pan-sharpened QUICKBIRD satellite imagery, aids in viewing cultural features or vegetation near and within the higher slope areas.

Figures 15, 18, 19, and 20 illustrate geologic setting, satellite imagery, and slope maps at study site 12, an area that locally has undeveloped terrain within the Del Rio clay and Buda limestone outcrop belt. The imagery illustrates contrasting vegetation of Del Rio clay and

Buda limestone at some places within the undeveloped terrain. Satellite imagery that has resolution sufficient to identify characteristic vegetation types can be used with detailed maps of ALTM data to aid in the mapping of geologic units. For example, figure 18 shows that a line of contrasting vegetation marks the contact between the Del Rio and Buda Formations. Figure 19 shows mapped areas having different slopes within Del Rio clay. Figure 20 highlights the areas of higher slopes, between 10° and 44°, that may be generally more prone to slope failure within this study site. High-resolution imagery is also useful for identifying cultural features. The location of higher slope areas can be compared with locations of roads and houses, as well as with the occurrence of undeveloped areas.

MAPPING STREAM TERRACES

ATLM data, used with high-resolution imagery, can greatly aid mapping of different stream terraces and channels along potential flood-prone areas within expanding suburban settings. Subdividing different terraces sometimes can be difficult because of vegetation covering the units and subtle changes in topography between some terraces. Figures 21 through 24 illustrate geologic setting, a detailed ground-elevation contour map, imagery, and maps of alluvium and terraces deposits for study site 13 along Onion Creek in southeast Austin. Combining the detailed ground-elevation contour map with high-resolution imagery allowed for a subdivision of the terrace deposits that was more detailed than the one done during previous mapping. For this example, ground-elevation contour maps having 2- and 3-ft contour intervals were studied using high-resolution imagery. Detailed maps such as the examples in figures 23 and 24 can provide basic information that is useful for planning land use and suburban development.

MAPPING FAULTS

Analysis of ATLM data is useful for recognizing local topographic expressions that reflect faults within hilly limestone terrain. For analysis of lidar data and faults at study site 14 (fig. 25), detailed ground-elevation contour maps, having contours between 2 and 5 ft, were constructed from lidar data and were compared with fault locations previously mapped by Garner and others (1976) along part of the Mount Bonnell fault, a major series of normal fault strands that bound the west edge of the Edwards aquifer recharge zone. This fault is one of the larger displacement faults of the Balcones Fault Zone. At this study site Cretaceous Edwards limestone and dolomitic limestone are downthrown against Cretaceous Glen Rose limestone, dolomitic limestone, and argillaceous limestone (fig. 25). Suburban development has encroached on the hilly limestone terrain of the study site, disturbing some of the natural topography and vegetation patterns (fig. 26). The study site lies along a part of the Mount Bonnell fault that contains several large-scale fault splays.

Figures 26 and 27 illustrate imagery of the study site and a ground-elevation contour map with previously mapped faults. Strata discontinuities caused by faulting display topographic expressions that aid in mapping faults. Sometimes these features are subtle. For example, figure 27 shows that mapped faults tend to (1) cut through topographic lows between hill tops

(often referred to as saddles) and (2) flank hillsides. An area of subtle linear topography, identified through the analysis of lidar data, aligns with a previously mapped fault and may indicate fault or fault-related fracture continuation that was not recognized during previous mapping by Garner and others (1976).

SUMMARY

1. ALTM data and high-resolution imagery are effective tools for mapping dolines in karst limestone terrain, high slope areas within deposits prone to slope failure, terraces of flood-prone streams, and faults in hilly limestone terrain. The ability to accurately map these geologic elements is important and often required for managing karst limestone aquifers and for planning land use and urban and suburban development in Central Texas and elsewhere. Lidar data allow for detailed analyses of ground elevation and slope variations. To meet mapping needs, these data can be studied with high-resolution imagery that illustrates natural and cultural features.
2. ALTM data allow for the mapping of subtle closed topographic depressions as small as 5 ft in width, as well as larger topographic depressions, within karst limestone terrain. These data can greatly aid ground-based mapping of dolines by providing remotely sensed interpretations of subtle features across large or site-specific areas of sometimes rugged terrain.
3. Analysis of ATLM data, high-resolution imagery, and geologic map data allows for the mapping of higher slope areas within clay-rich strata that are prone to slope failure and foundation problems. ATLM data can be used to accurately subdivide clay-rich strata areas on the basis of smaller to greater topographic slopes in order that areas that are more prone to slope failure can be identified.
4. ATLM data allow for the detailed mapping of stream terraces and channels through the analysis of detailed ground-elevation maps that can be studied using high-resolution imagery.
5. Analysis of ATLM data allows for the recognition of sometimes subtle, topographic expressions that reflect stratigraphic discontinuities caused by faulting. Study of detailed ground-elevation maps of a site within hilly limestone terrain shows that previously mapped faults cut through topographic lows between hilltops and flank hillsides. An area of subtle linear topography, identified through the analysis of lidar data, aligns with a previously mapped fault and may indicate fault or fault-related fracture continuation that was not recognized during previous mapping.

ACKNOWLEDGMENTS

This work was supported primarily by the NASA-AASG project that is administered by the California Institute of Technology, Jet Propulsion Laboratory. This work also benefited from previous airborne laser terrain mapping that was supported by the City of Austin and from previous and ongoing geologic mapping of Central Texas urban growth areas and aquifer recharge areas supported by the USGS-administered STATEMAP program. Nico Houwert, geologist for the City of Austin, provided a digital data set of karst features within the Edwards aquifer. Another digital data set of karst features in Central Texas was compiled through files at the Texas Environmental Quality Commission. Quickbird satellite imagery used for this study was provided by The University of Texas at Austin Center for Space Research. Graphics for this report was by Paula Beard and David M. Stephens, Lana Dieterich edited this report, and Jamie H. Coggin did the layout, all under the supervision of Joel L. Lardon, Media Services Department Interim Manager.

REFERENCES

Collins, E. W., and Woodruff, C. M., Jr., 2001, Faults in the Austin, Texas, area—defining aspects of local structural grain, *in* Woodruff, C. M., Jr., and Collins, E. W., Trip Coordinators, 2001, Austin, Texas, and beyond—geology and environment: a field excursion in memory of L. Edwin Garner: Austin Geological Society Guidebook 21, p. 15–26.

Garner, L. E., and Young, K. P., 1976, Environmental geology of the Austin area: an aid to urban planning: The University of Texas at Austin, Bureau of Economic Geology Report of Investigations No. 86, 39 p. + pls.

Garner, L. E., Young, K. P., Rodda, P. U., Dawe, G. L., and Rogers, M. A., 1976, Geologic map of the Austin area, Texas, *in* Garner, L. E., and Young, K. P., 1976, Environmental geology of the Austin area: an aid to urban planning: The University of Texas at Austin, Bureau of Economic Geology Report of Investigations No. 86, scale 1:65,500, plate VII.

Hill, R. T., 1900, Physical geography of the Texas region: U.S. Geological Survey, Folio 3(T), 12 p. + pls.

Tremblay, T. A., and Andrews, John, 1997, Digital data set for geologic map of the Austin, Texas, area: The University of Texas at Austin, Bureau of Economic Geology Open-File Digital Data Set.

Woodruff, C. M., Jr., 1975, Land capability in the Lake Travis vicinity, Texas, a practical guide for the use of geologic and engineering data: The University of Texas at Austin, Bureau of Economic Geology Report of Investigations No. 84, 37 p.

Woodruff, C. M., Jr., and Collins, E. W., Trip Coordinators, 2001, Austin, Texas, and beyond—geology and environment: a field excursion in memory of L. Edwin Garner: Austin Geological Society Guidebook 21, 120 p.

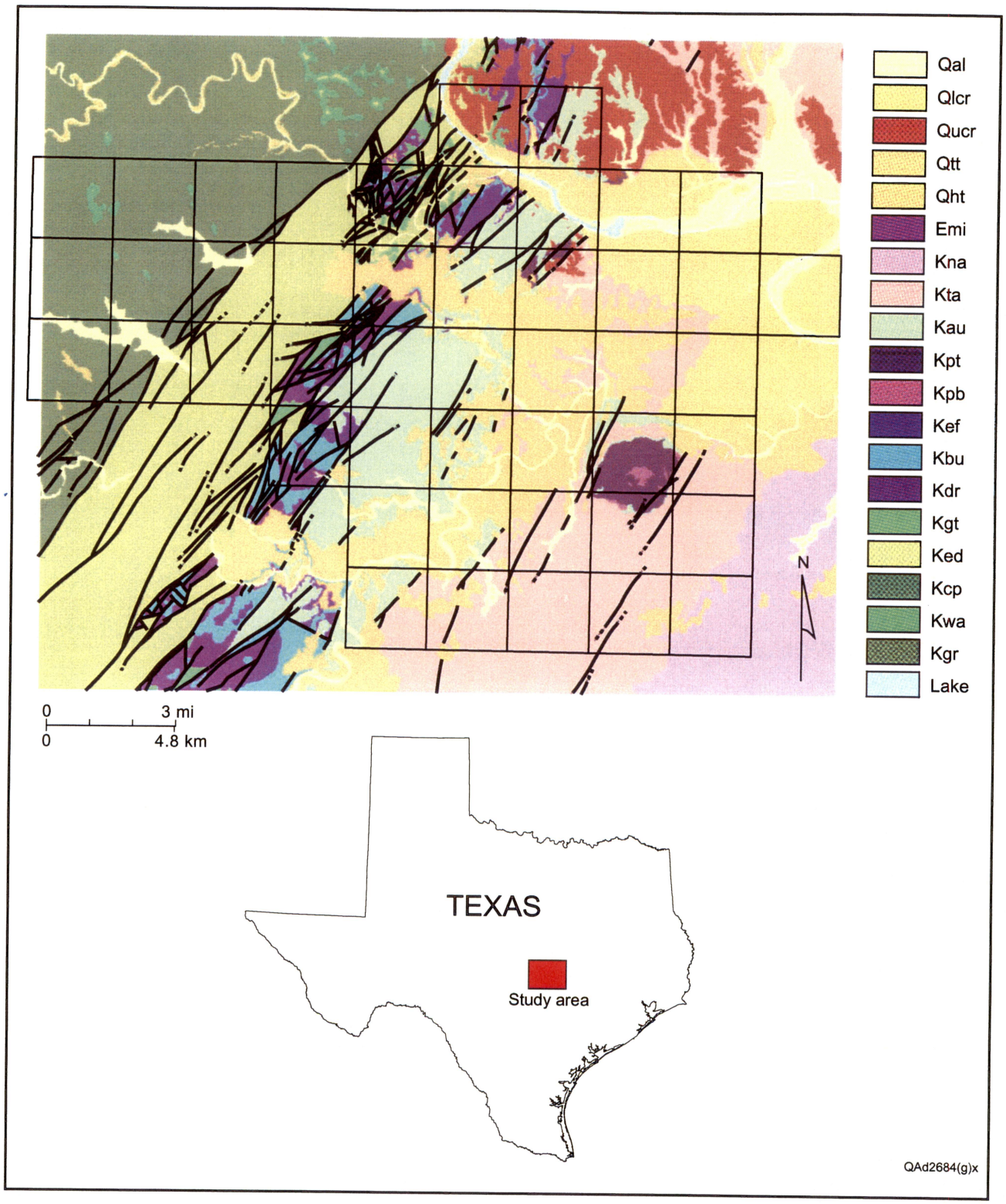

Figure 1. Geology of south Austin, Texas, region. Geology from digital geologic map data set (Tremblay and Andrews, 1997) constructed from *Geologic Map of the Austin, Texas, Area* (Garner and others, 1976). Tiles indicate areas of airborne lidar data. Study sites described in this report are within Cretaceous Glen Rose (Kgr), Edwards (Ked), Del Rio (Kdr), Buda (Kbu), and Eagle Ford (Kef) units and Quaternary terrace deposits (Qtt).

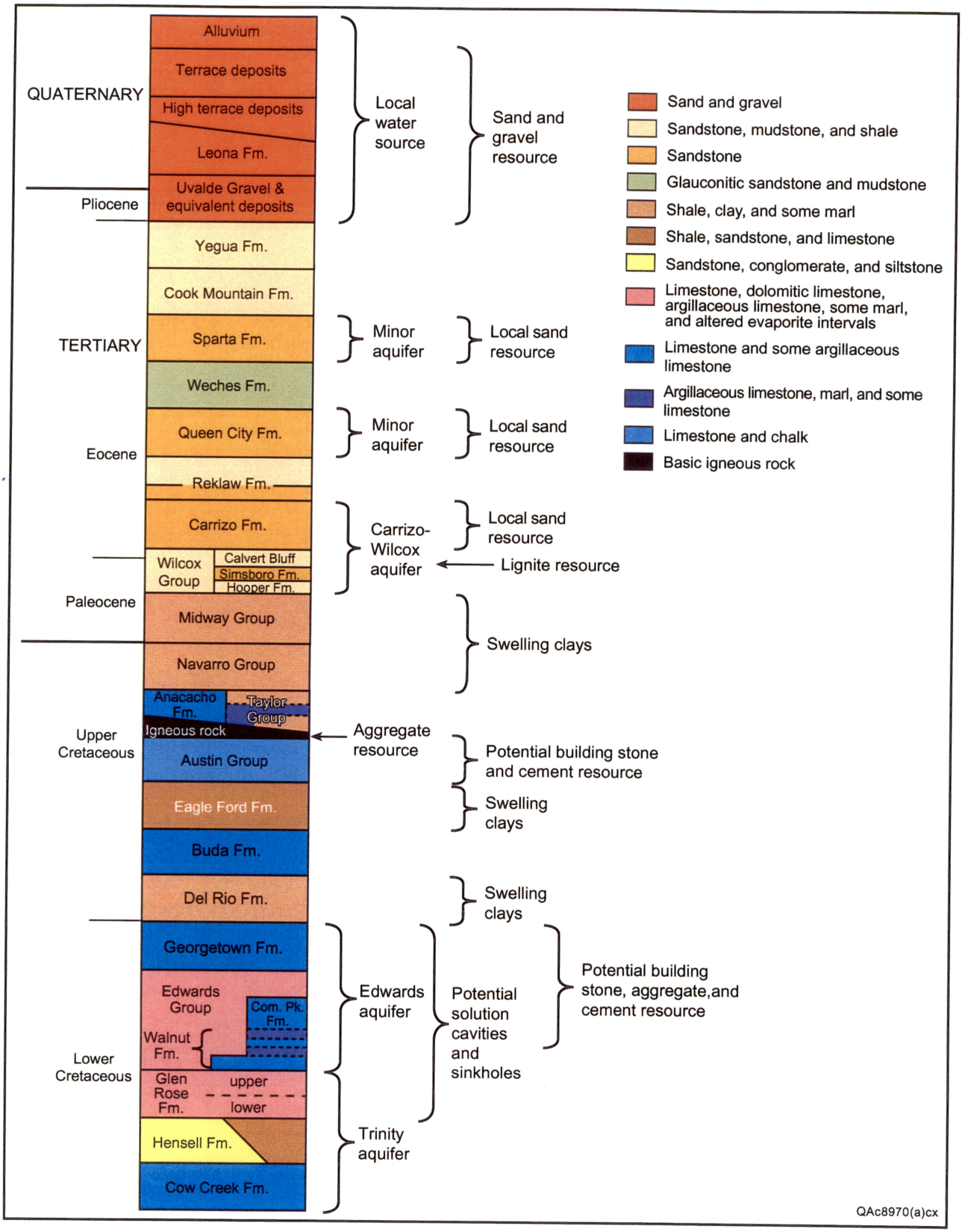

Figure 2. General stratigraphic column and Earth resources of Central Texas. Study sites described in this report are within Cretaceous Glen Rose, Edwards, Del Rio, Buda, Eagle Ford units and Quaternary terrace deposits.

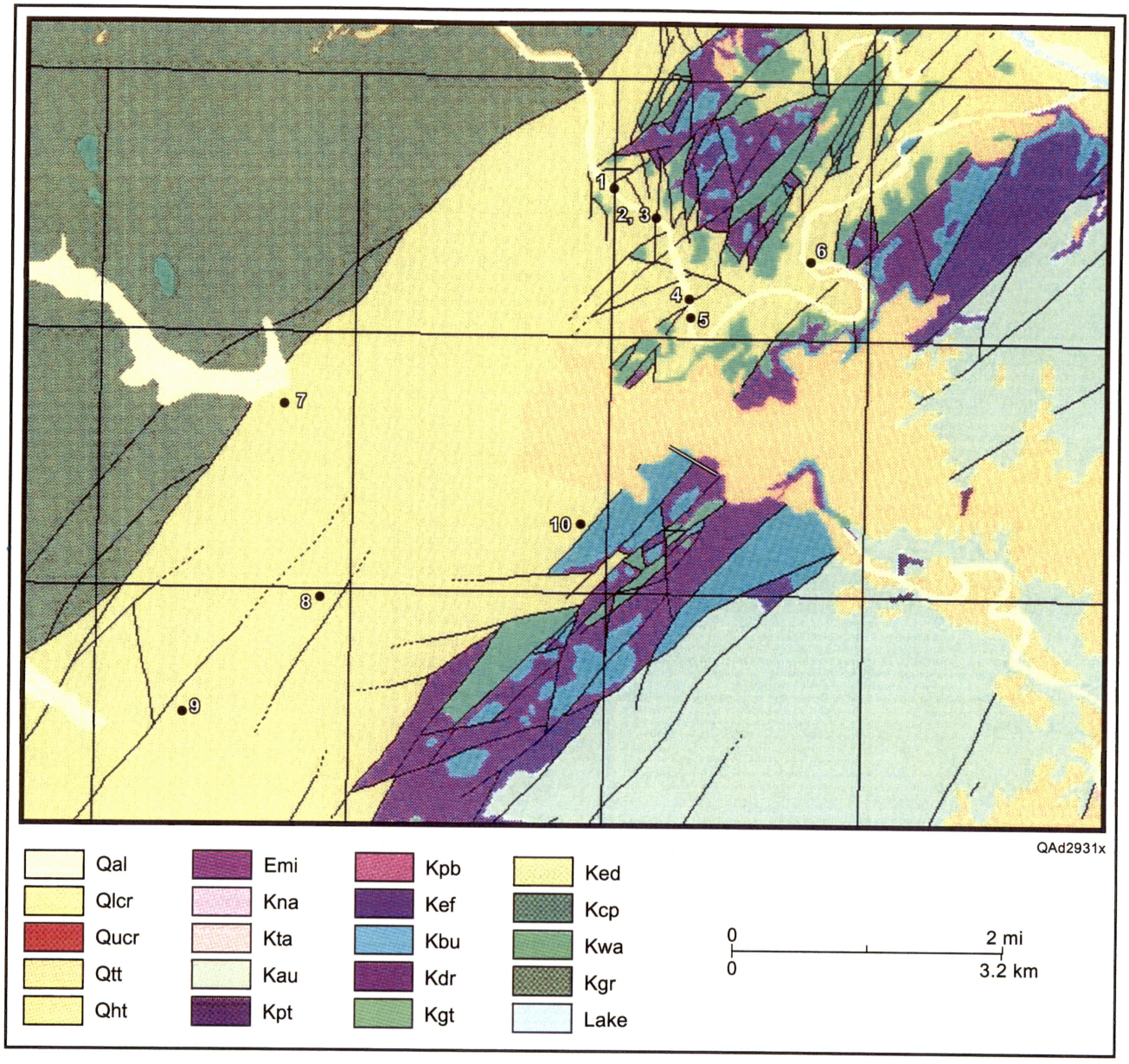

Figure 3. Geologic setting and location of study sites 1 through 10 for mapping dolines and closed-topographic depressions within the recharge zone of Edwards aquifer. Geology from digital geologic map data set (Tremblay and Andrews, 1997) constructed from Geologic Map of the Austin, Texas, Area (Garner and others, 1976). Tiles indicate areas of airborne lidar data. The study sites are within limestone and dolomitic limestone of the Edwards unit (Ked).

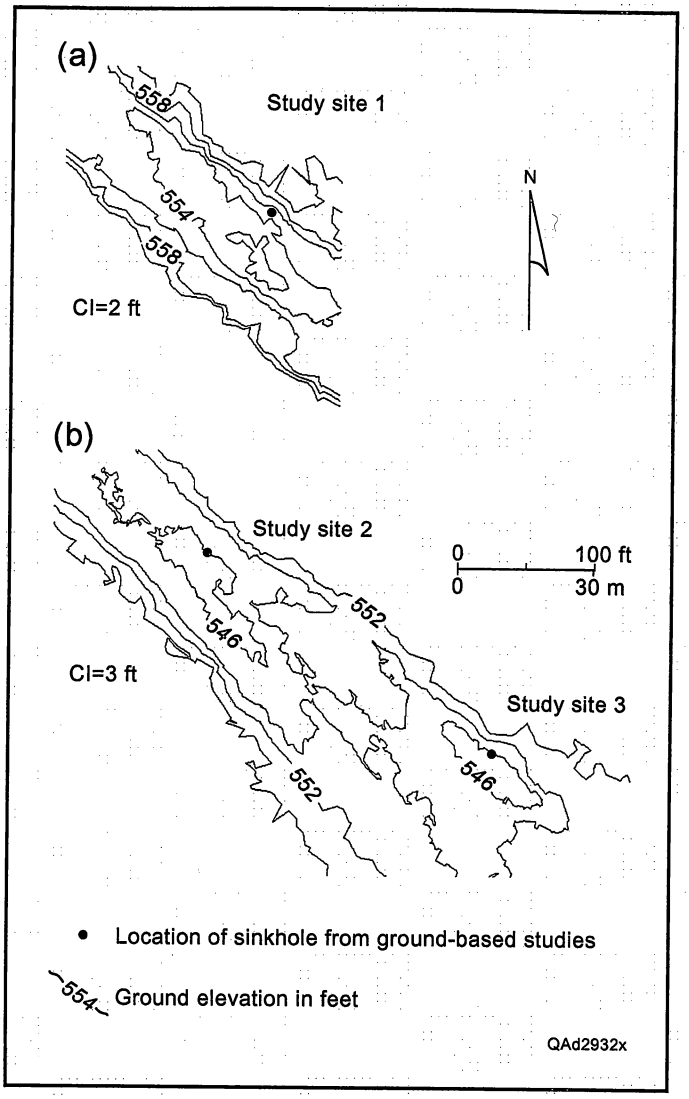

Figure 4. Topographic maps constructed from lidar data for (a) study site 1 and (b) study sites 2 and 3. Remotely sensed, closed topographic depressions correspond to locations of sinkholes mapped from ground-based studies [City of Austin Karst Data Base (Nico Houwert, personal communication, 2003)].

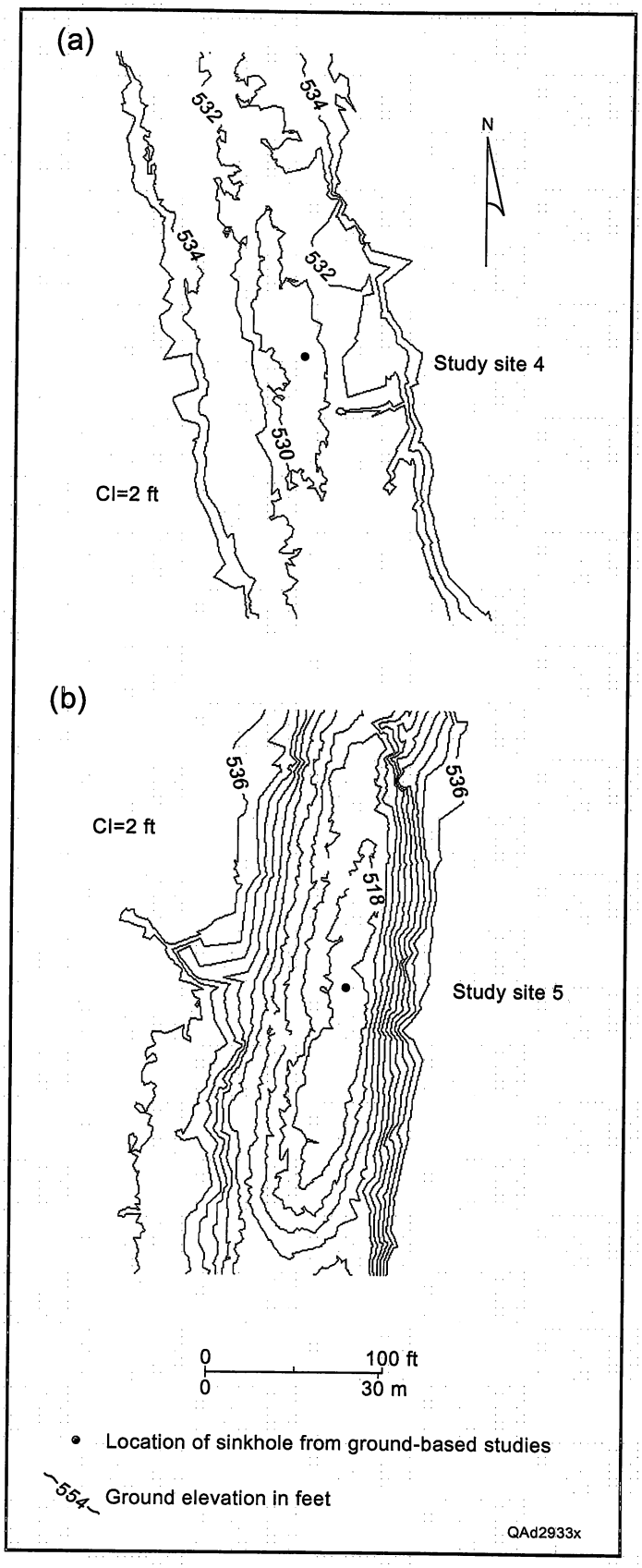

Figure 5. Topographic maps constructed from lidar data for (a) study site 4 and (b) study site 5. Remotely sensed, closed topographic depressions correspond to locations of sinkholes mapped from ground-based studies [City of Austin Karst Data Base (Nico Houwert, personal communication, 2003)].

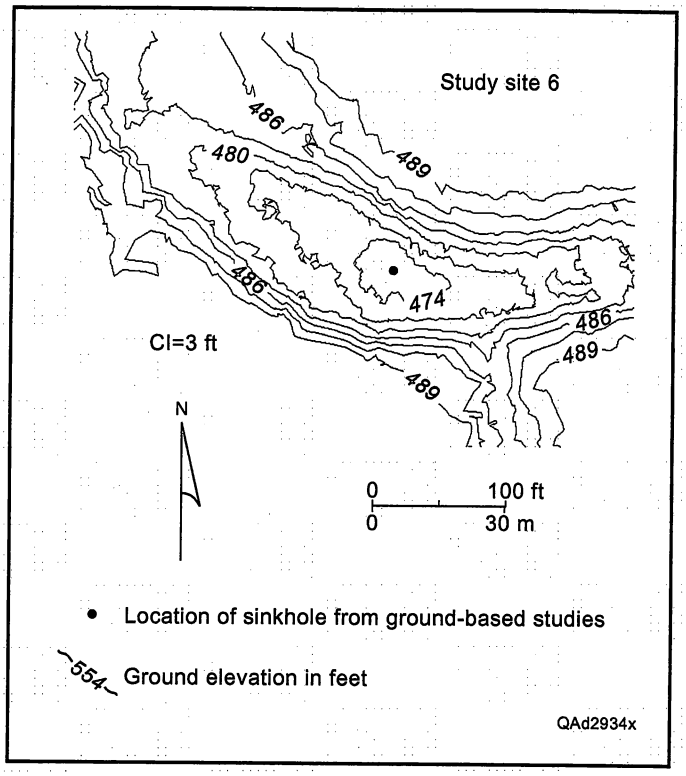

Figure 6. Topographic map constructed from lidar data for study site 6. Remotely sensed, closed topographic depression corresponds to location of sinkhole mapped from ground-based studies (David Johns, City of Austin Geologist, personal communication, 2001.

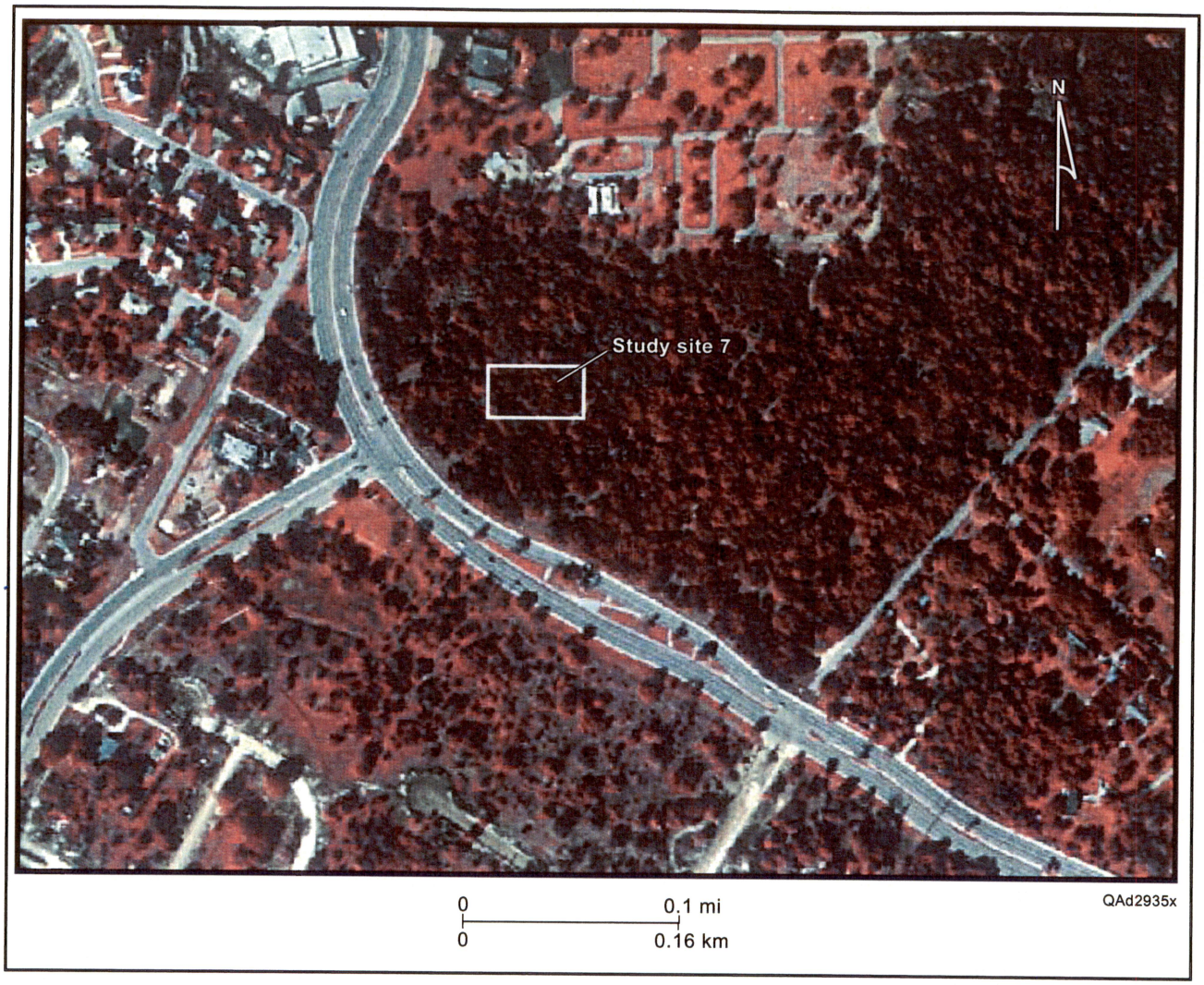

Figure 7. Aerial photograph showing setting of study site 7 within the Edwards aquifer recharge zone.

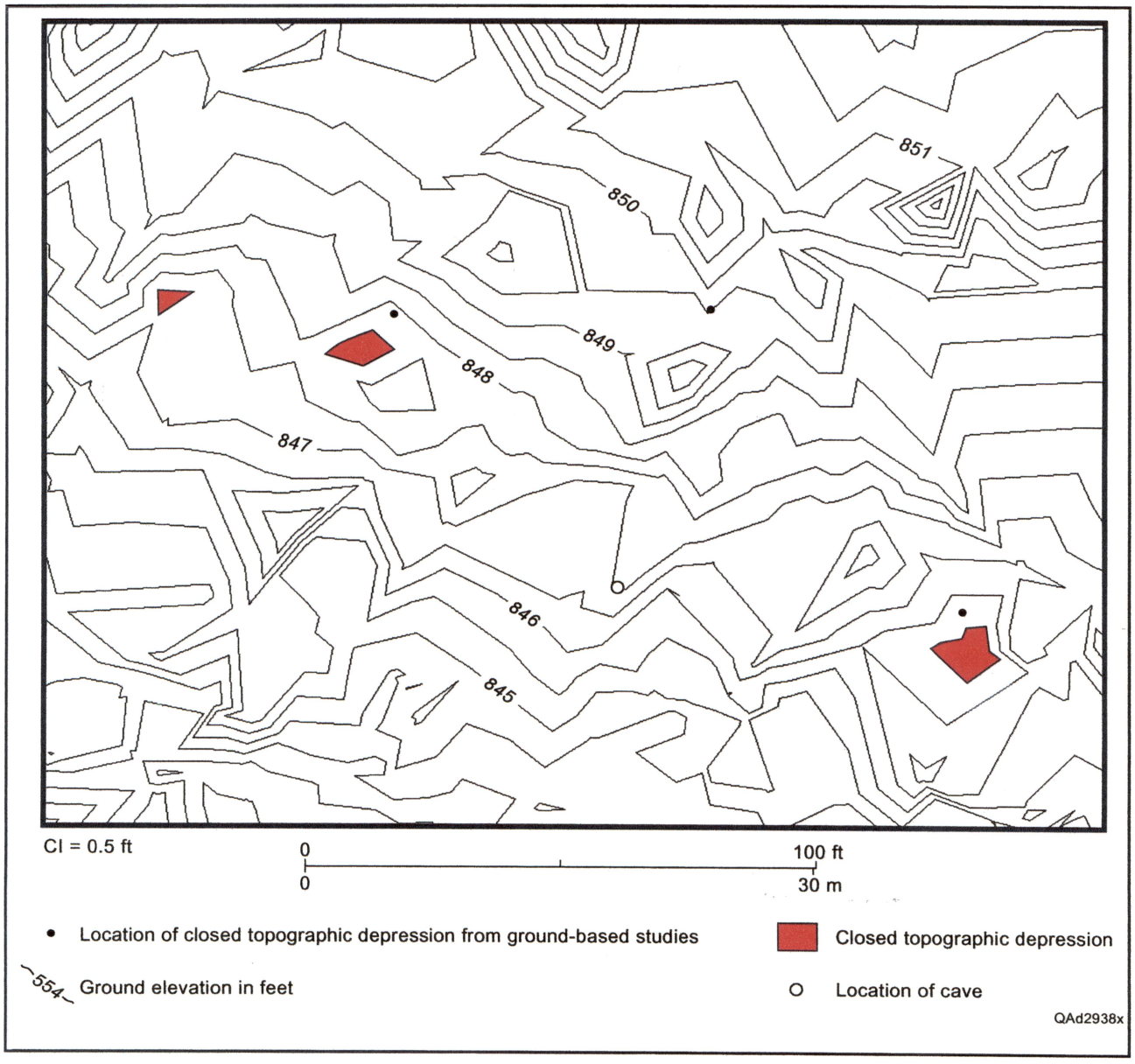

Figure 8. Topographic map constructed from lidar data for study site 7 within the Edwards aquifer recharge zone. Locations of two closed-topographic depressions identified from ground-based studies [Central Texas Geological Assessment database (Jennifer Rawlings and Adrien Lindley, personal communication, 2003)] are close to subtle, closed-topographic depressions mapped from the lidar data. Other features identified from ground-based studies show no apparent topographic expression on the topographic map constructed from lidar data.

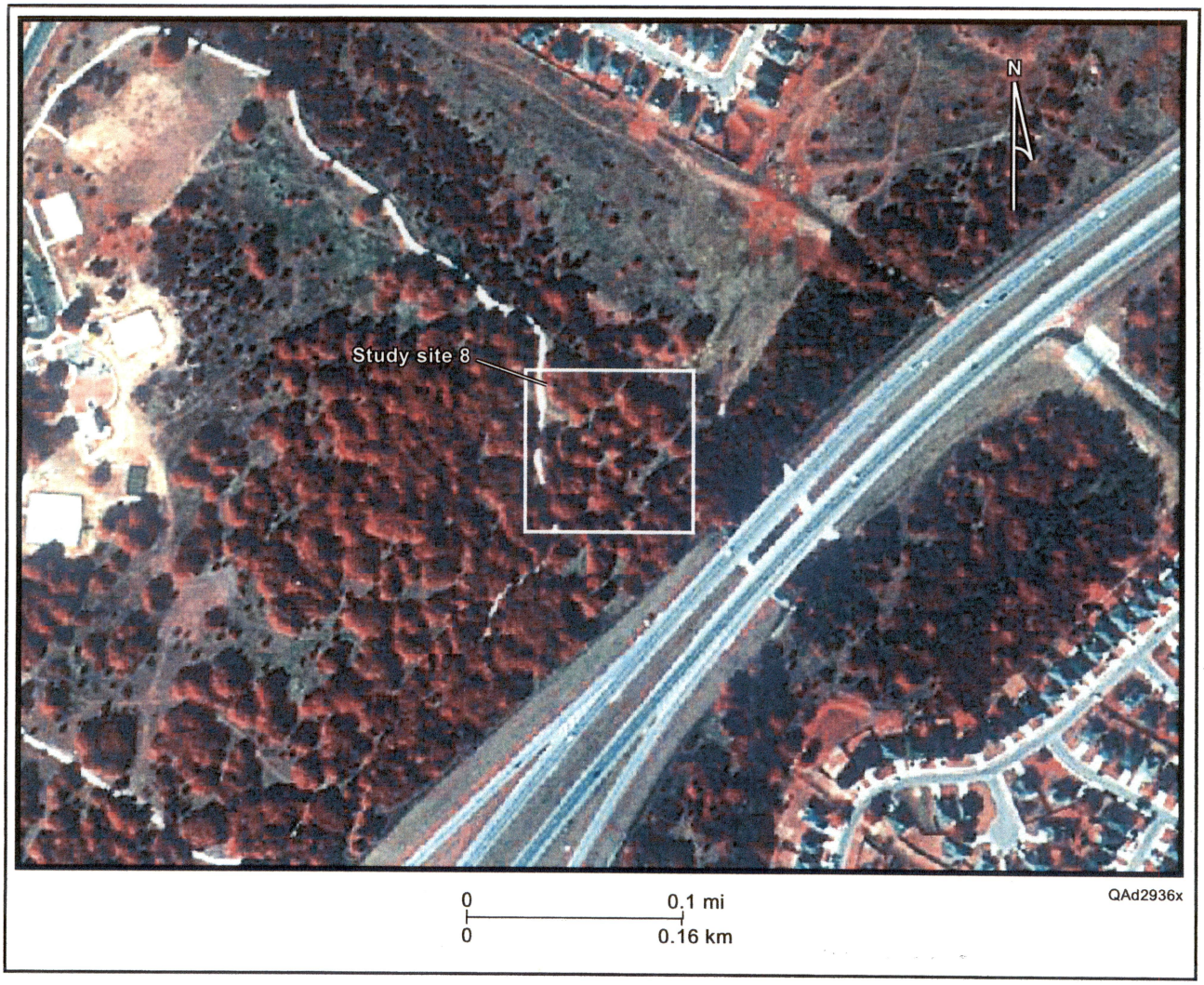

Figure 9. Aerial photograph showing setting of study site 8 within the Edwards aquifer recharge zone.

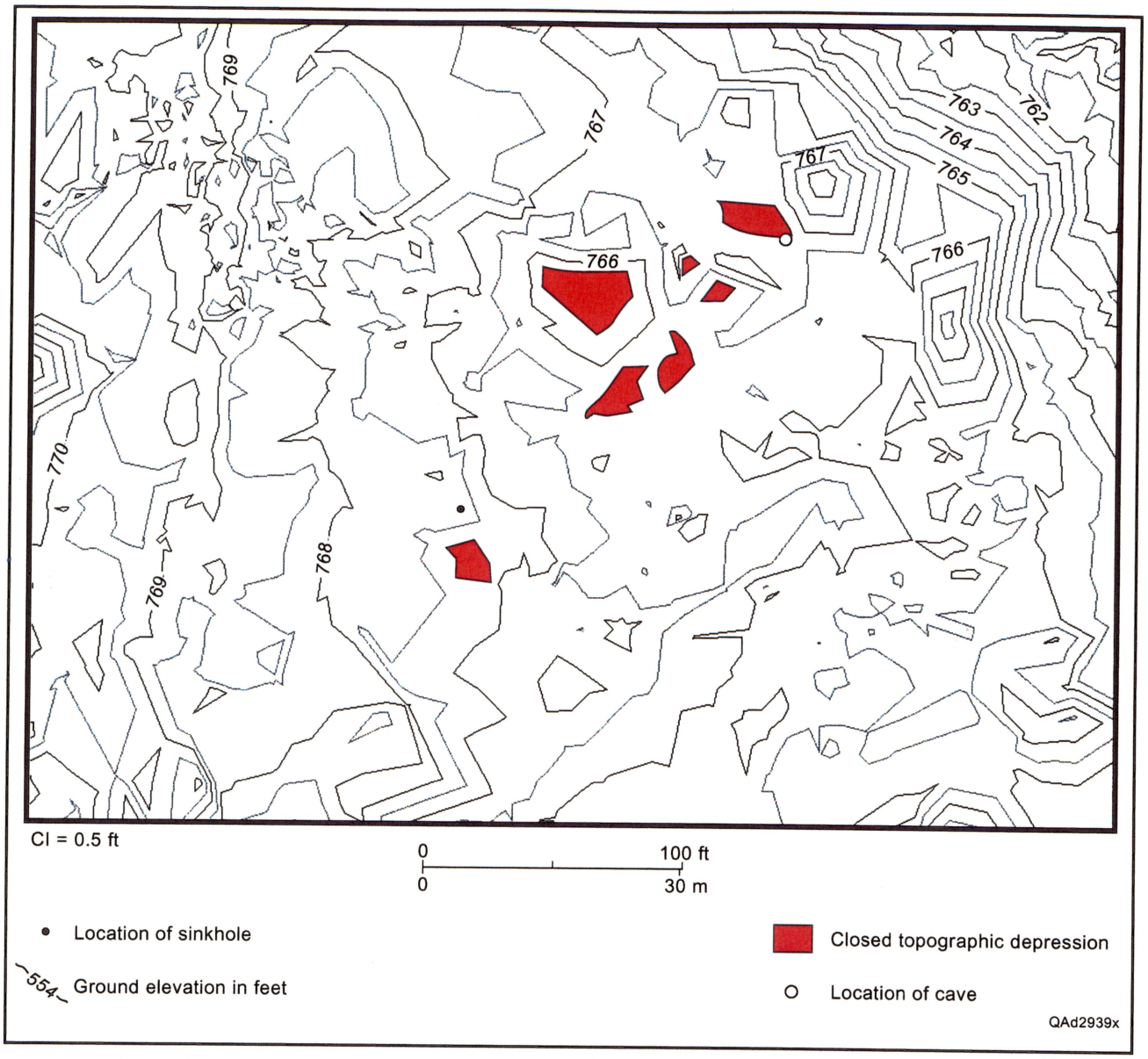

Figure 10. Topographic map constructed from lidar data for study site 8 within the Edwards aquifer recharge zone. Locations of a sinkhole and cave identified from ground-based studies [City of Austin Karst Data Base (Nico Houwert, personal communication, 2003); Central Texas Geological Assessment database (Jennifer Rawlings and Adrien Lindley, personal communication, 2003)] are near several remotely sensed, closed topographic depressions.

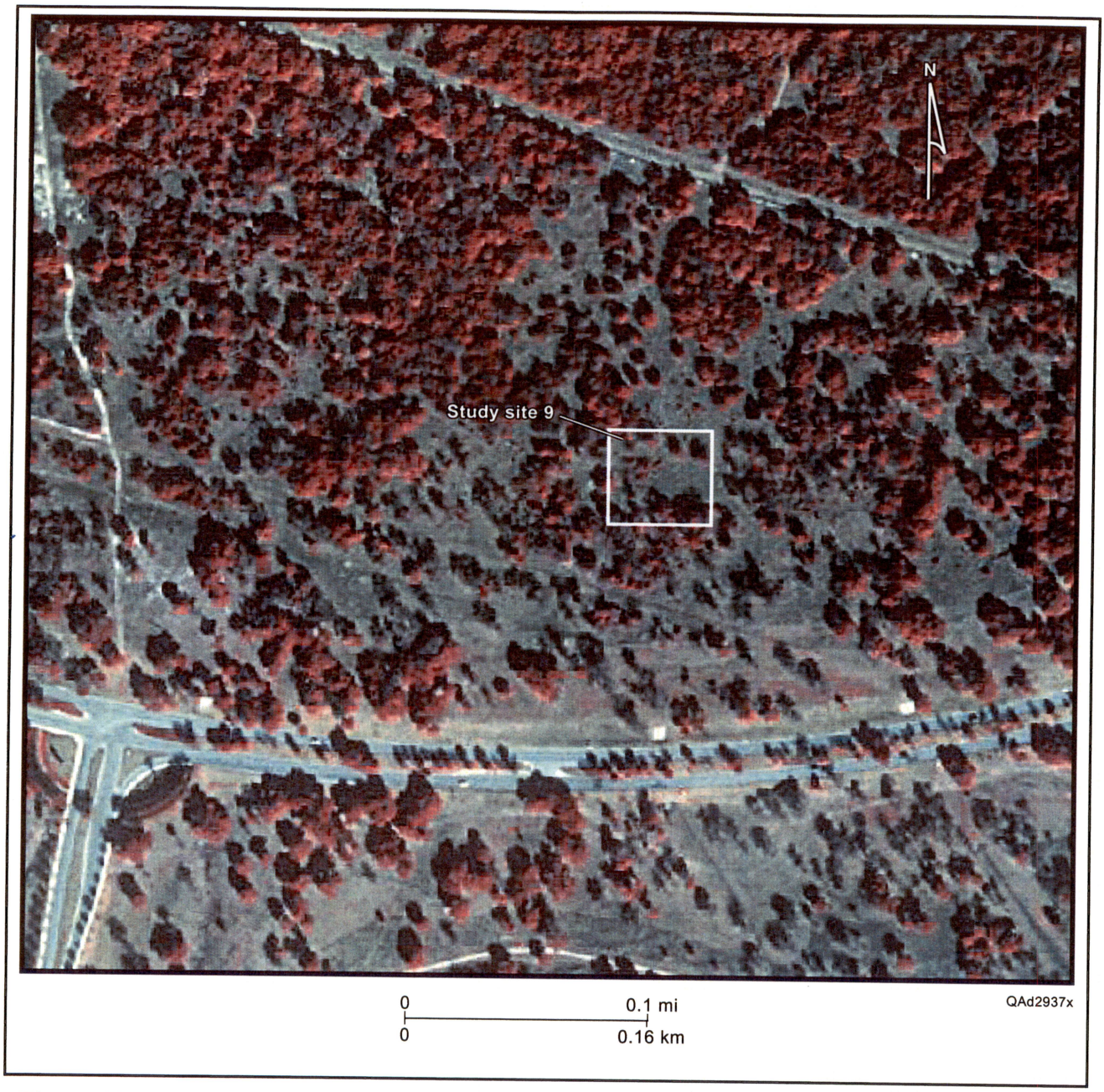

Figure 11. Aerial photograph showing setting of study site 9 within the Edwards aquifer recharge zone.

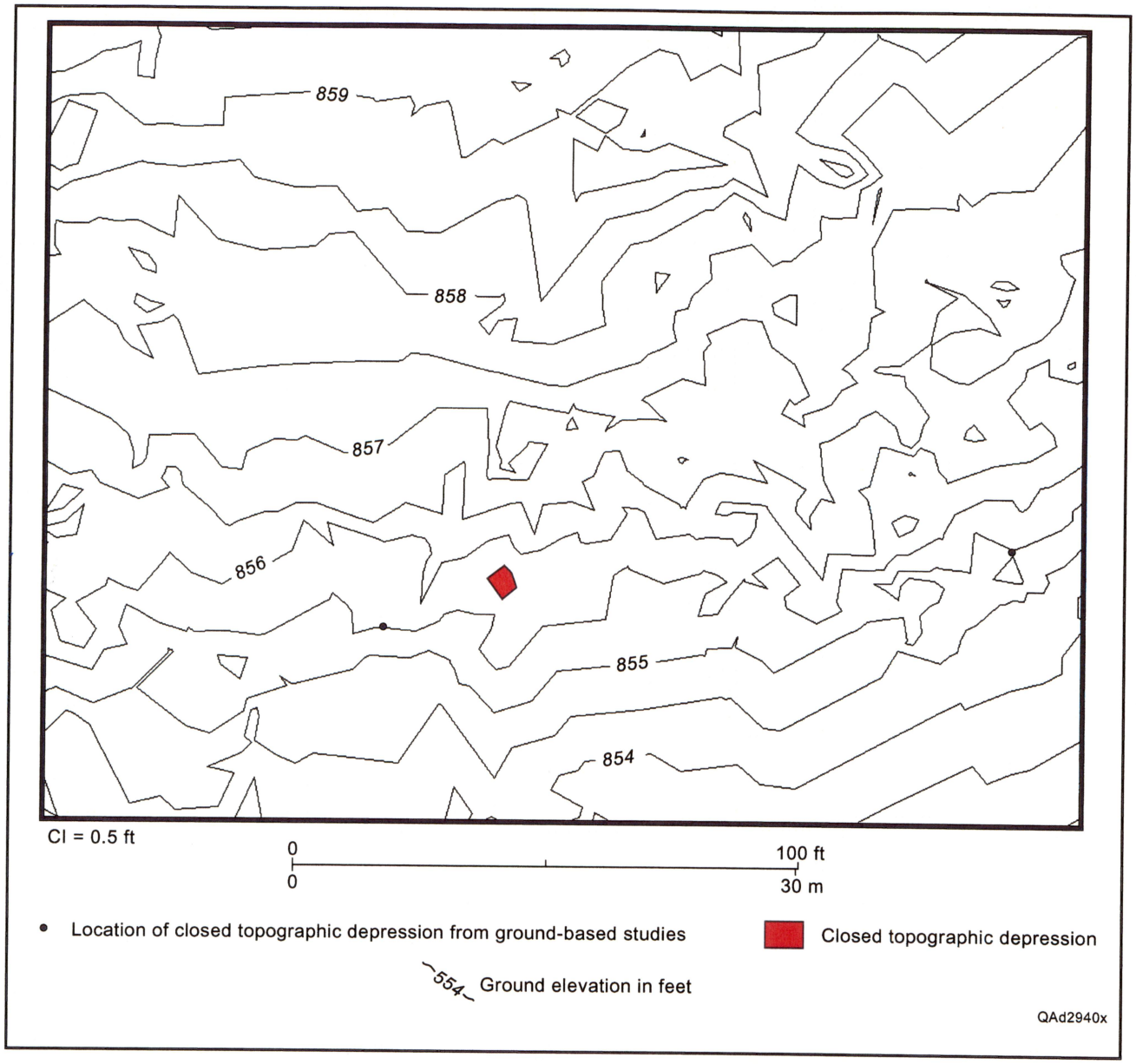

Figure 12. Topographic map constructed from lidar data for study site 9 within the Edwards aquifer recharge zone. Only one remotely sensed, closed topographic depression identified from the lidar data is in the vicinity of a closed topographic depression and an area of solution collapse identified through ground-based studies [Central Texas Geological Assessment database (Jennifer Rawlings and Adrien Lindley, personal communication, 2003)].

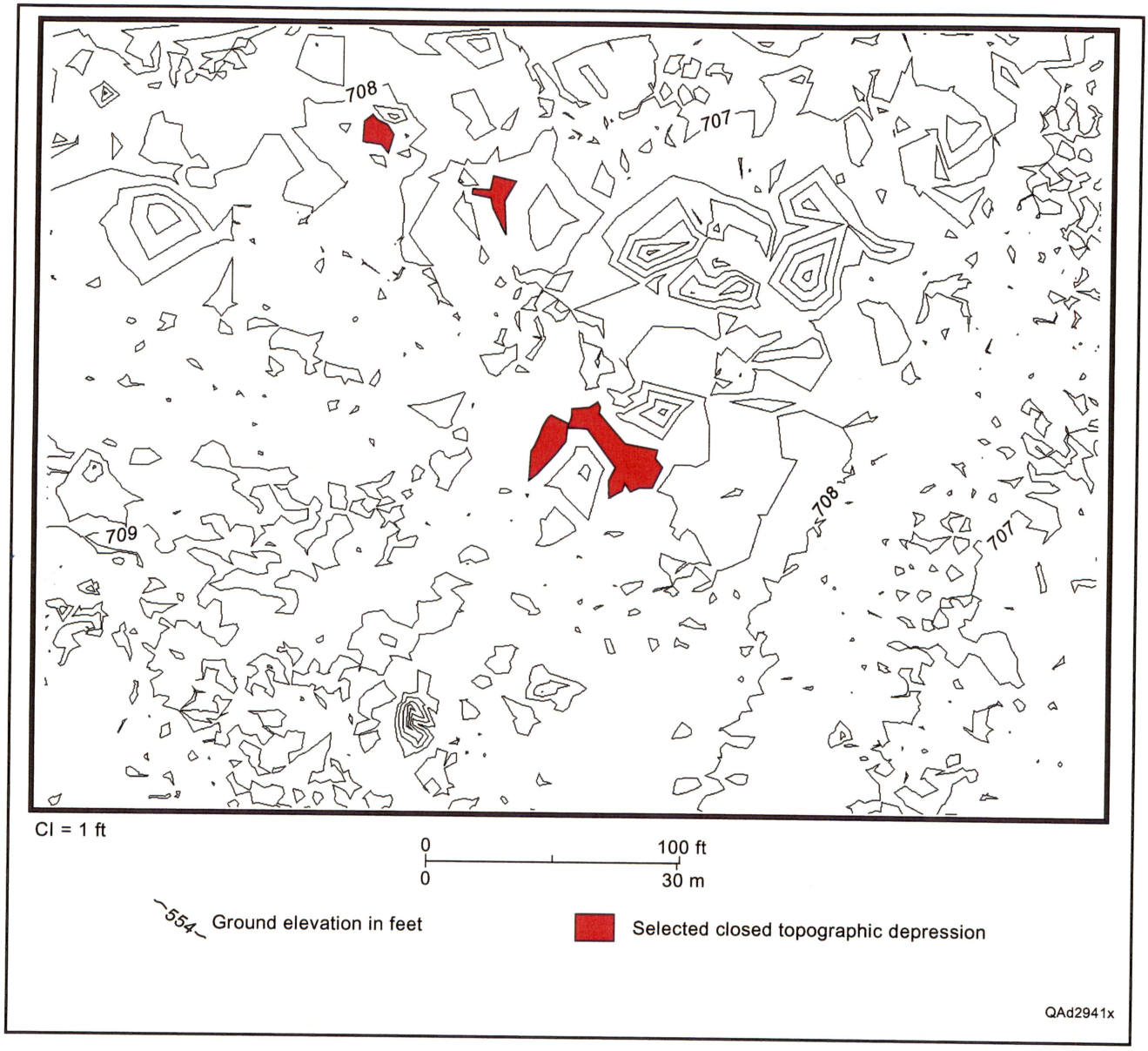

Figure 13. Topographic map constructed from lidar data for study site 10 within the Edwards aquifer recharge zone, which has not undergone ground-based studies for mapping karst features. Three remotely sensed, closed topographic depressions are identified from the lidar data. They are illustrated using high-resolution satellite imagery of the study site in figure 14.

Figure 14. Location of selected, remotely sensed, closed topographic depressions at study site 10 that are superimposed on high-resolution, pan-sharpened QUICKBIRD satellite imagery. The remotely sensed, closed topographic depressions were identified from the topographic map constructed from lidar data shown in figure 13.

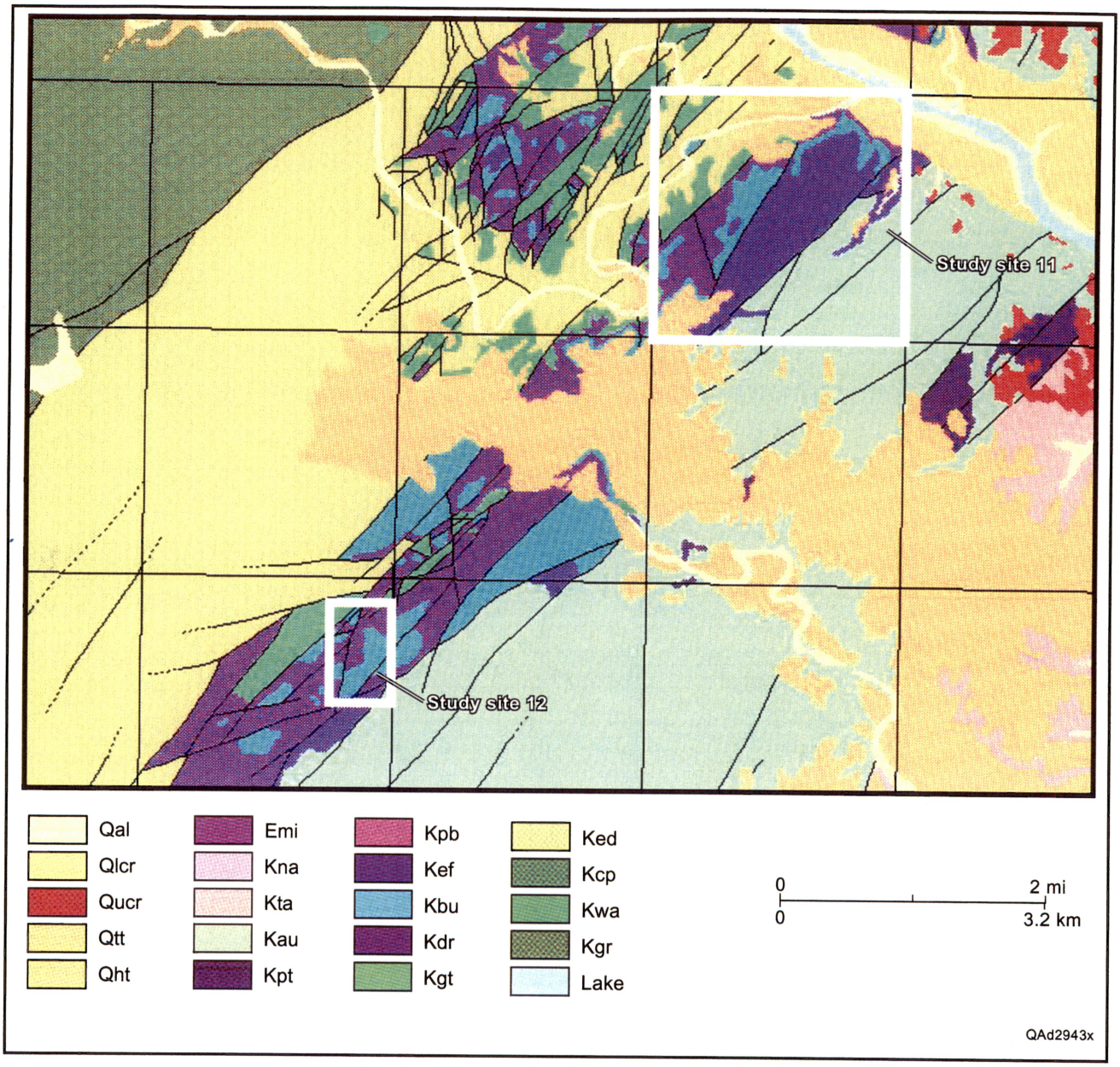

Figure 15. Geologic setting and location of study sites 11 and 12 within the Del Rio-Buda-Eagle Ford Formations outcrop belt. Geology from digital geologic map data set (Tremblay and Andrews, 1997) constructed from *Geologic Map of the Austin, Texas, Area* (Garner and others, 1976). Tiles indicate areas of airborne lidar data. Kdr—Del Rio Formation; Kbu—Buda Formation; Kef—Eagle Ford Formation.

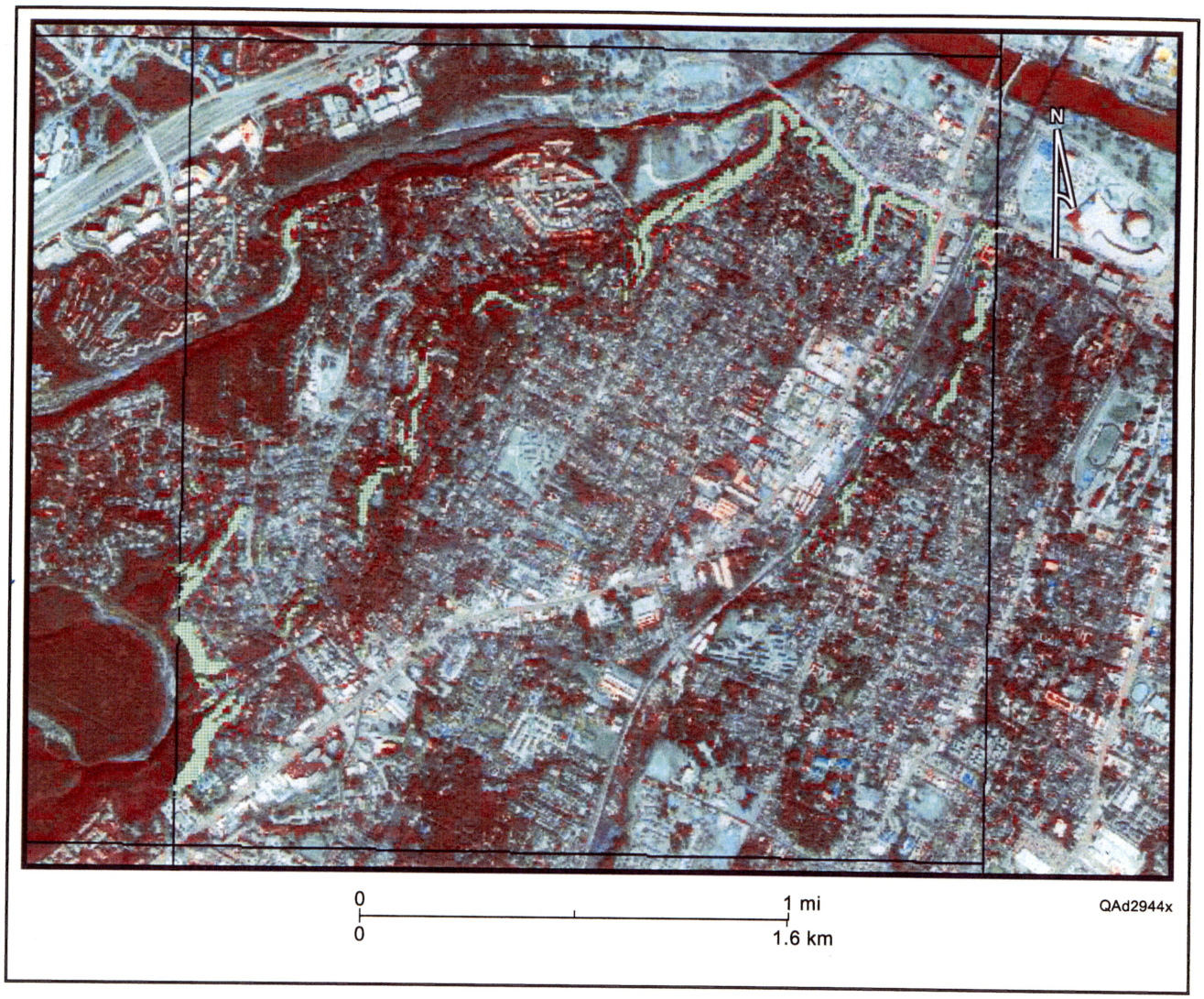

Figure 16. Areas mapped within the Del Rio-Buda-Eagle Ford Formations at study site 11 that have ground slopes between 12° and 52° (patterned area). These higher slope areas are superimposed on a QUICKBIRD satellite image for visualization of natural and cultural features. In general, higher slope areas within this clay-rich stratal sequence may be more prone to slope failure and foundation problems than lower slope areas. Geologic setting shown in figure 15.

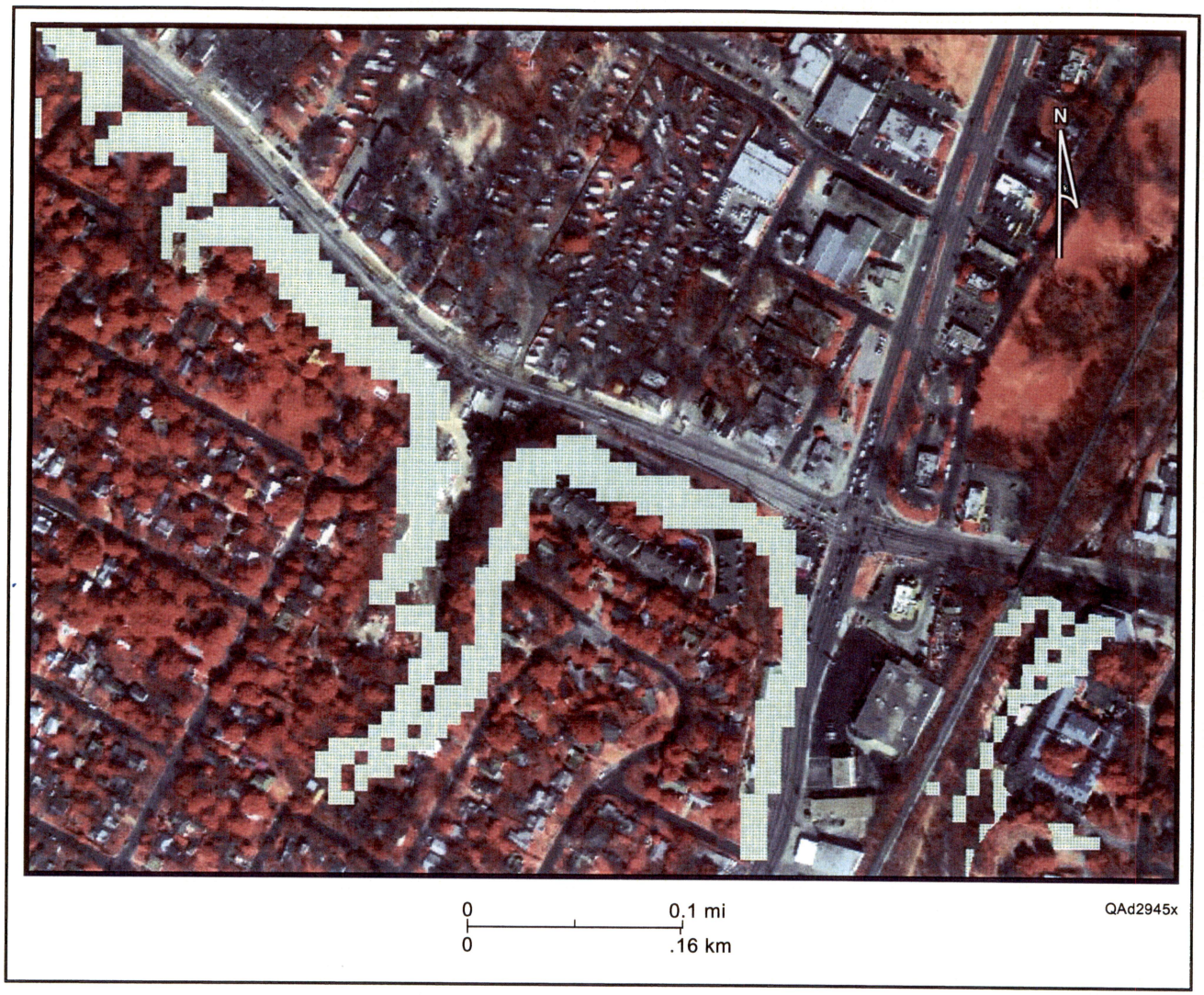

Figure 17. Close-up of areas mapped within the Del Rio-Buda-Eagle Ford Formations in the northeast part of study site 11 that have ground slopes between 12° and 52° (patterned area). These higher slope areas are superimposed on a pan-sharpened, high-resolution QUICKBIRD satellite image for visualization of natural and cultural features. Geologic setting shown in figure 15.

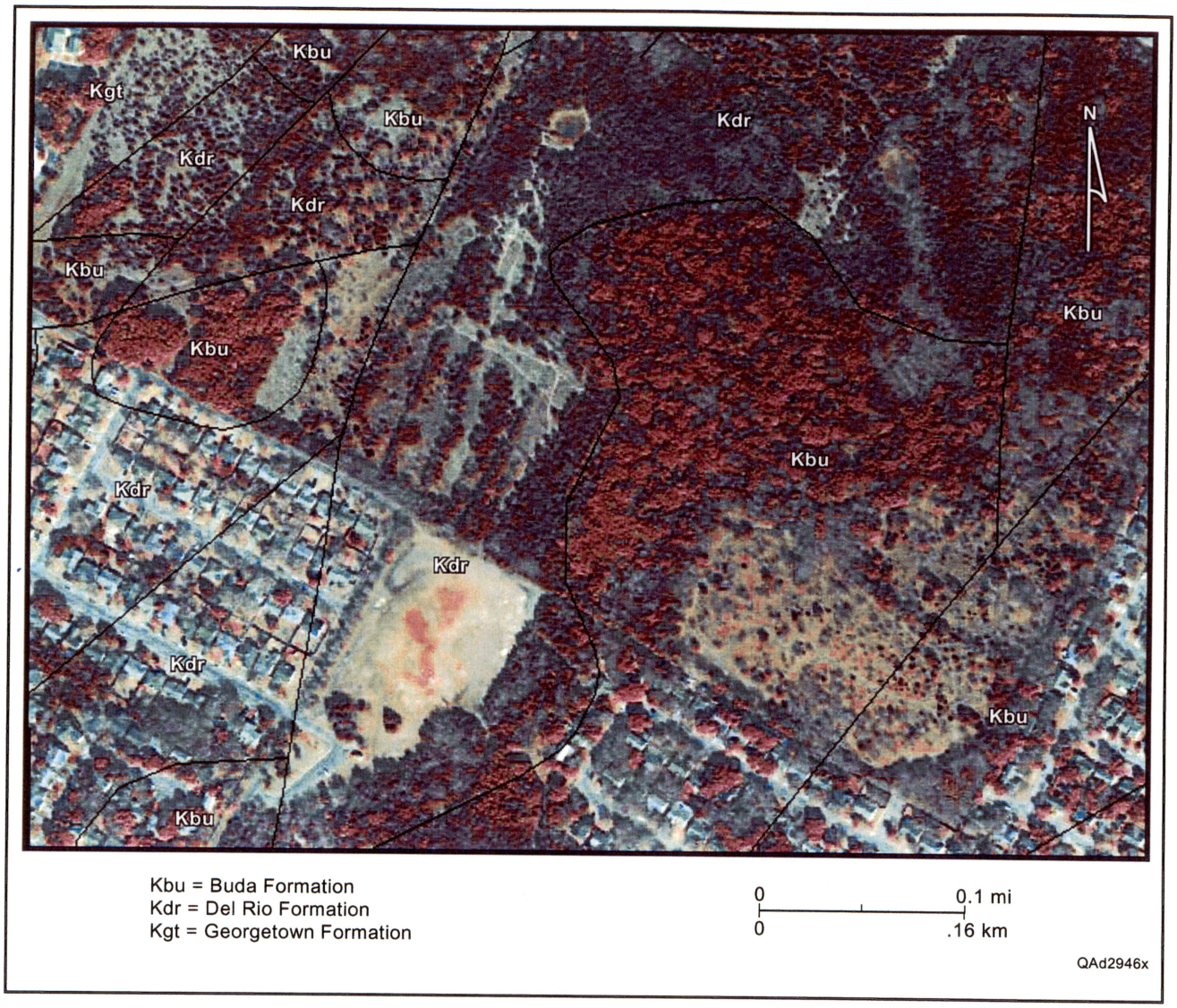

Figure 18. Geology of study site 12 within the Del Rio-Buda-Eagle Ford Formations outcrop belt. Geology is superimposed on a pan-sharpened, high-resolution QUICKBIRD satellite image for visualization of natural and cultural features. Geologic setting shown in figure 15.

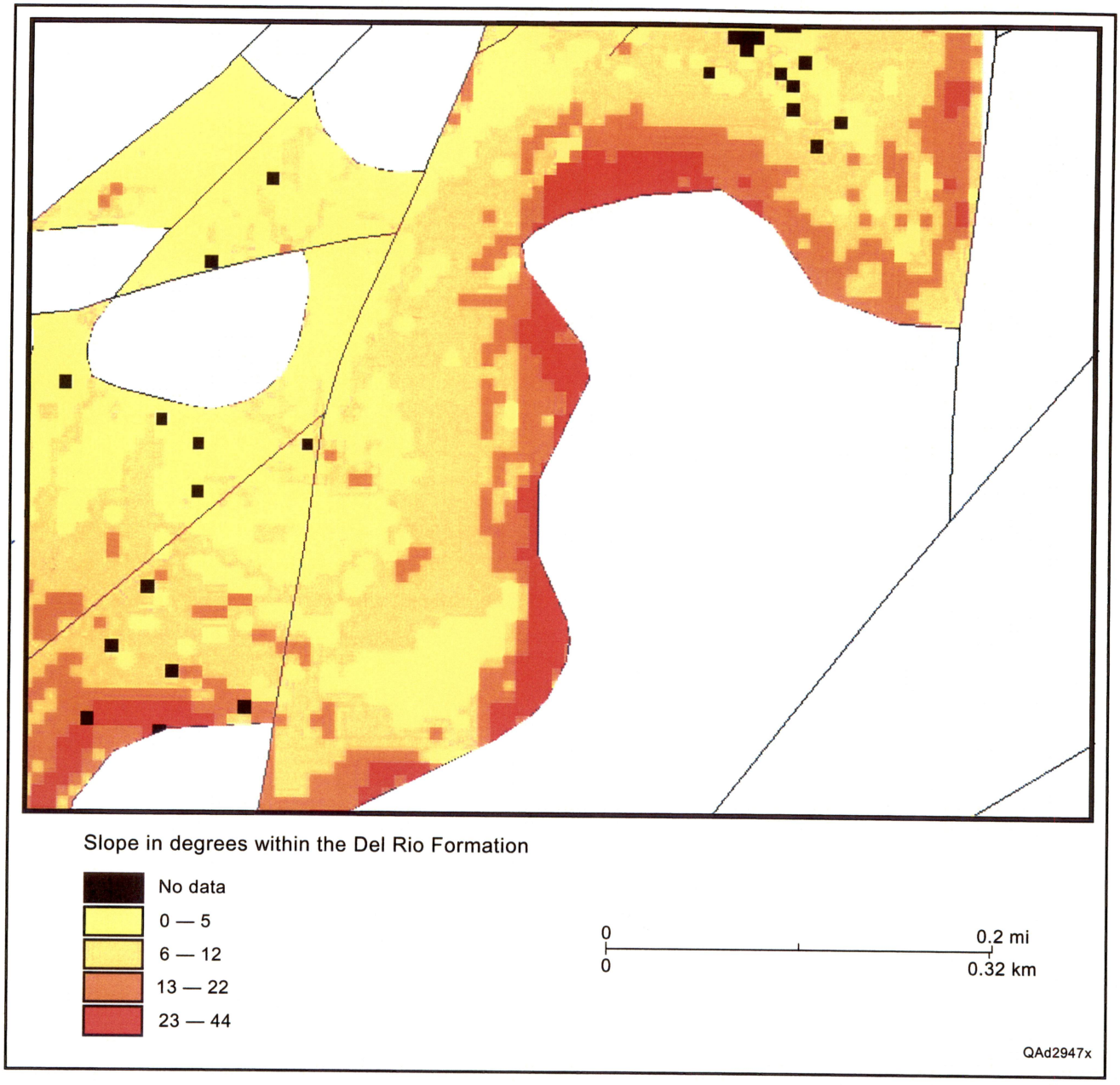

Figure 19. Mapped areas at study site 12 having different ground slopes within Del Rio clay. In general, higher slope areas within this clay-rich unit may be more prone to slope failure and foundation problems than lower slope areas. Geologic setting shown in figure 15.

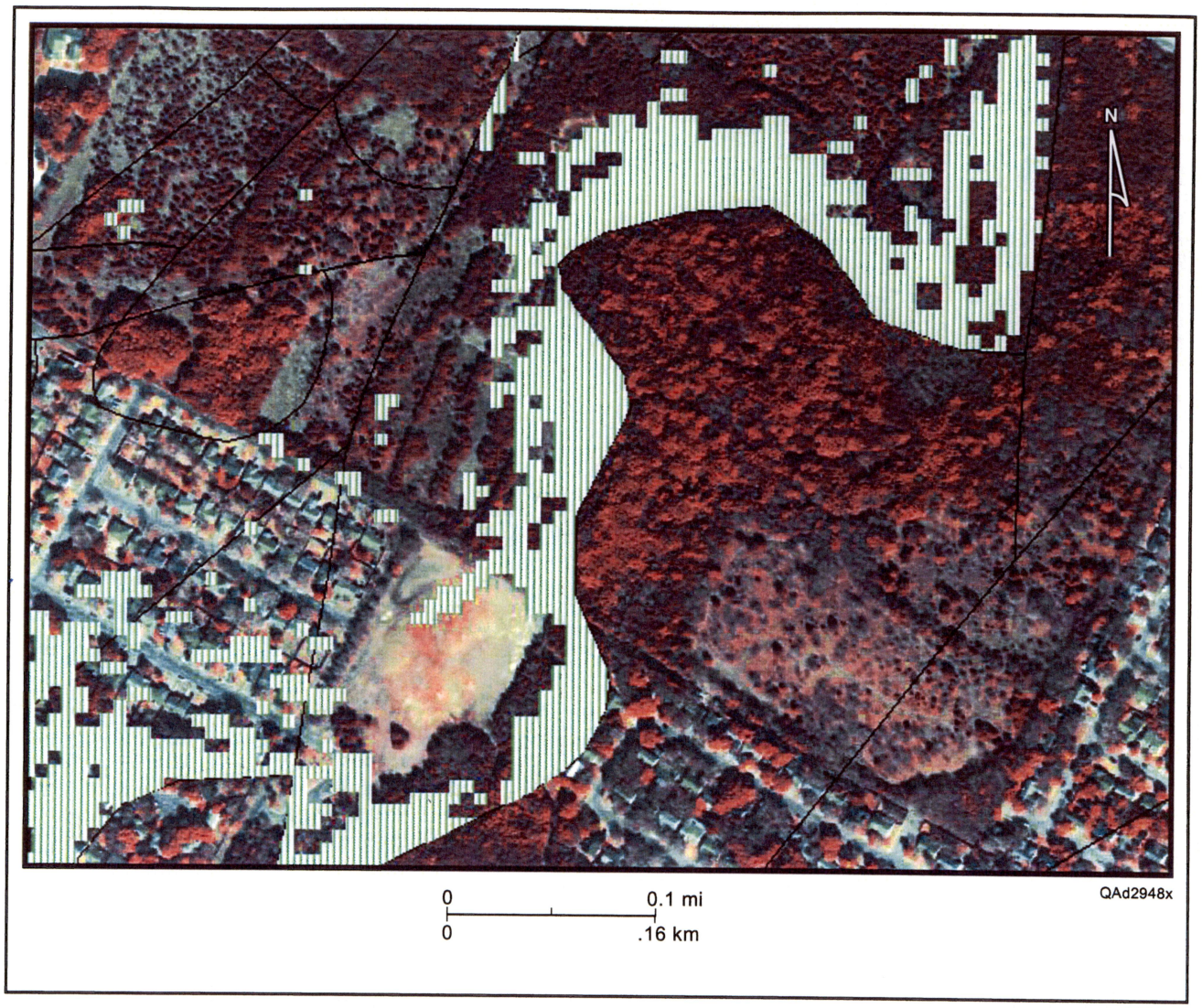

Figure 20. Mapped areas at study site 12 having ground slopes greater than 10° (patterned area) within Del Rio clay. These higher slope areas are superimposed on a pan-sharpened, high-resolution QUICKBIRD satellite image for visualization of natural and cultural features. In general, higher slope areas within this clay-rich unit may be more prone to slope failure and foundation problems than lower slope areas. Geologic setting shown in figure 15.

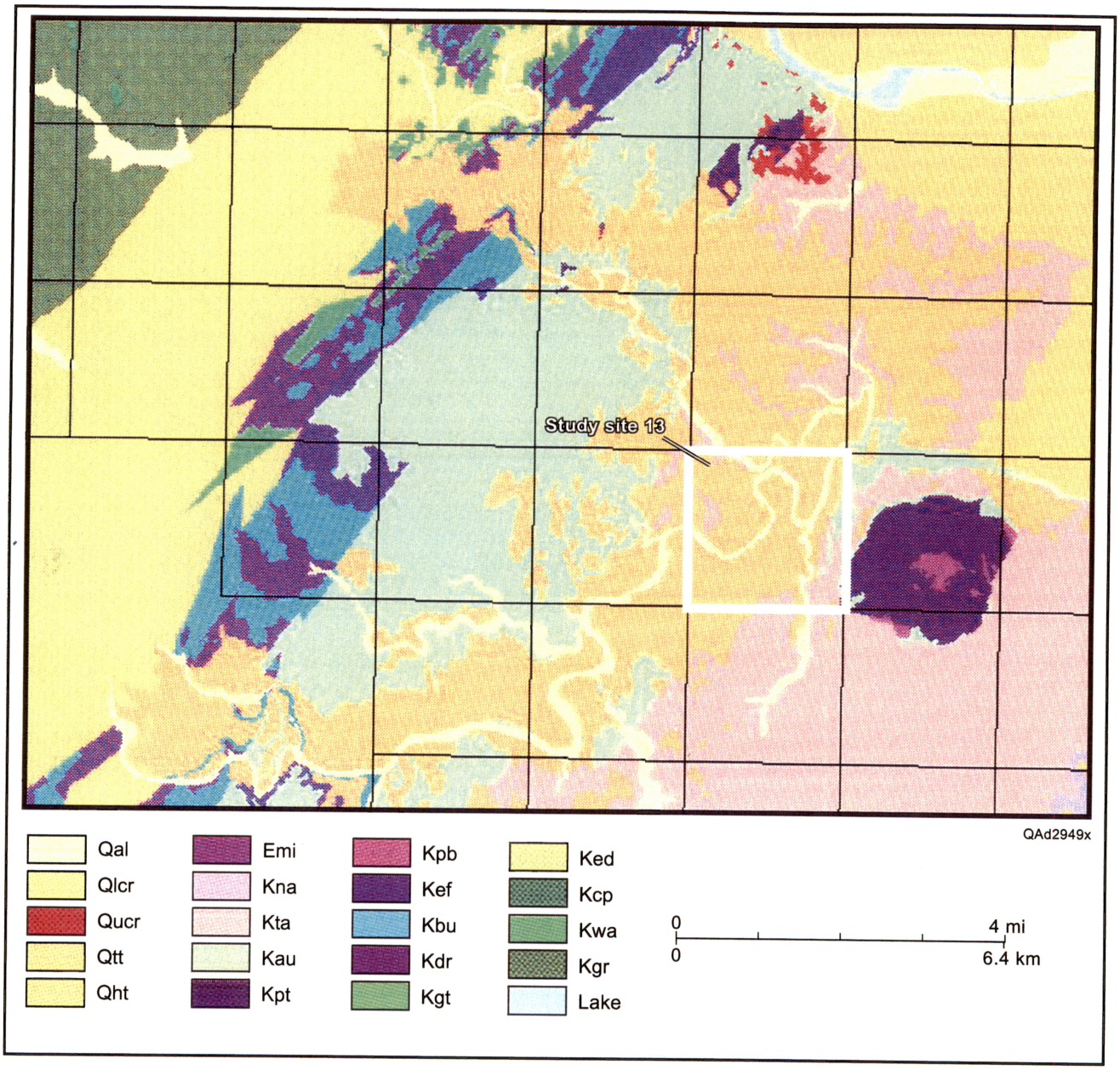

Figure 21. Geologic setting and location of study site 13 within terrace deposits (Qtt) of Onion Creek. Geology from digital geologic map data set (Tremblay and Andrews, 1997) constructed from *Geologic Map of the Austin, Texas, Area* (Garner and others, 1976). Tiles indicate areas of airborne lidar data.

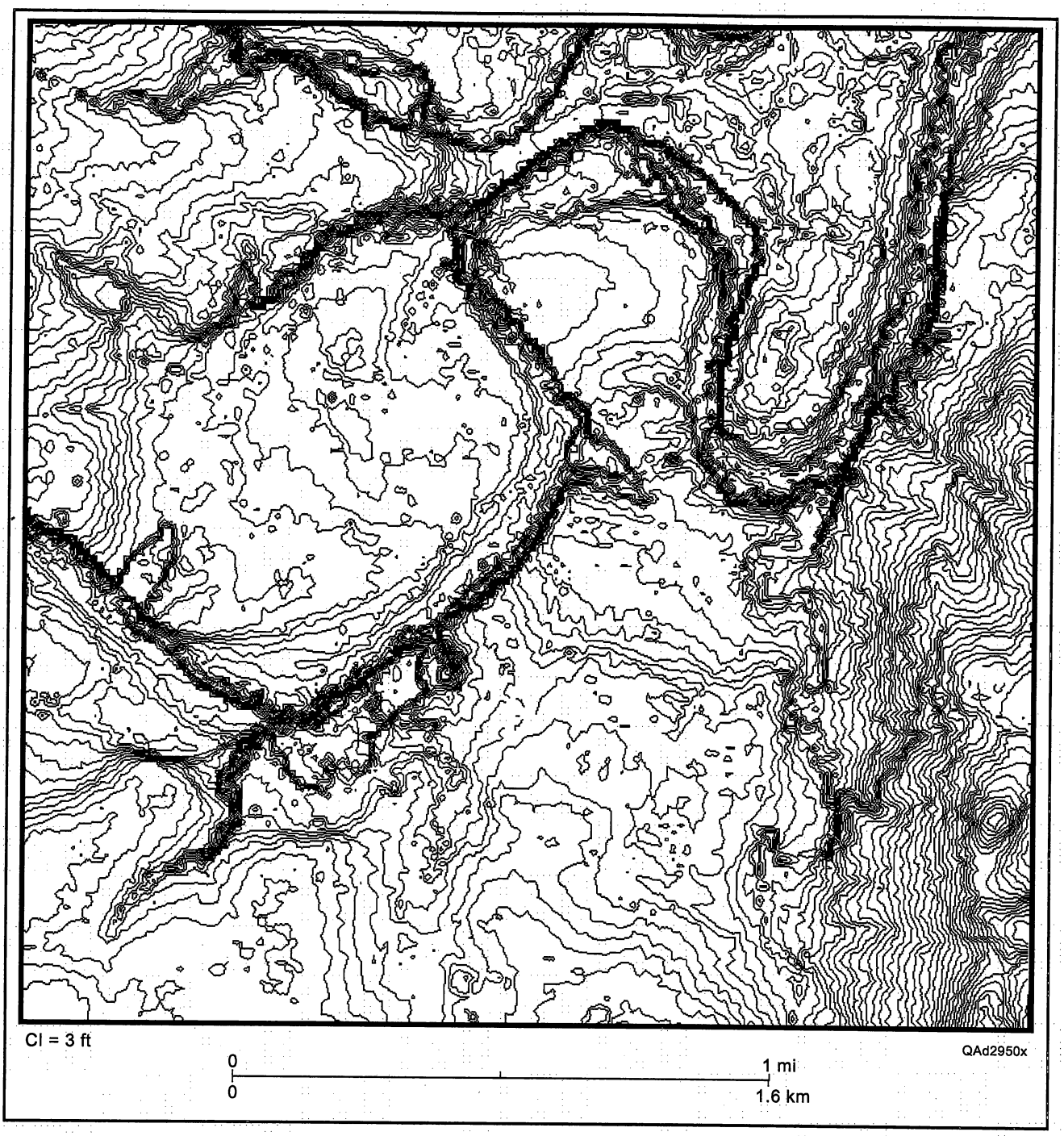

Figure 22. Detailed topographic map constructed from lidar data of study site 13, within terrace deposits of Onion Creek. Geologic setting shown in figure 21. Contour interval = 3 ft. Specific elevations available within digital data set.

Figure 23. Geologic map showing generalized subdivision of terrace deposits at study site 13. Generalized subdivision of terrace deposits was determined using detailed topography from lidar data and QUICKBIRD satellite imagery. Local areas of Cretaceous bedrock modified from Garner and others (1976). Geologic setting shown in figure 21.

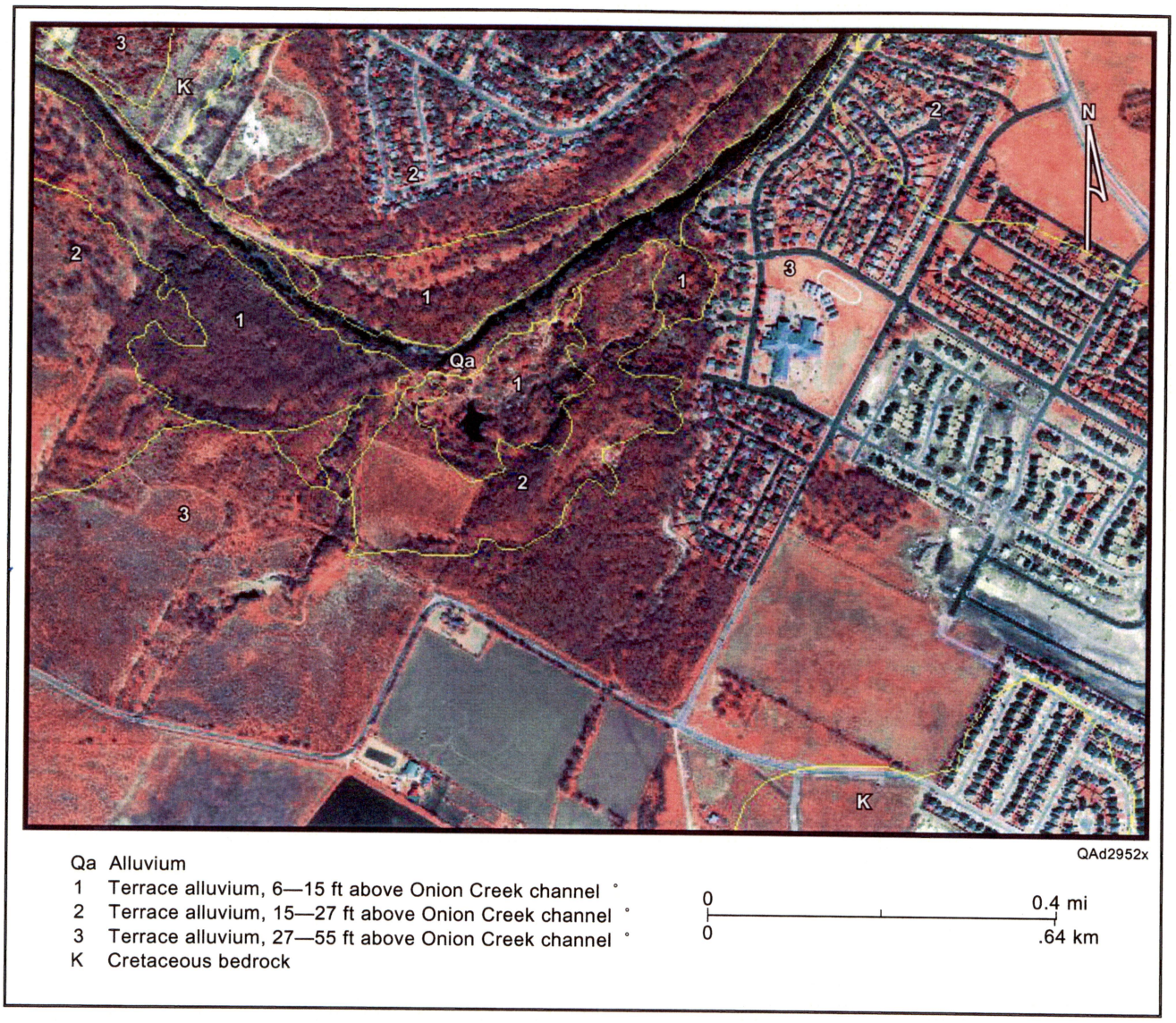

Figure 24. Close-up of geologic map showing generalized subdivision of terrace deposits at study site 13. Geology is superimposed on pan-sharpened, high-resolution QUICKBIRD satellite imagery. Geologic setting shown in figure 21. Qal—alluvium; Ked—Edwards Group; Kgr—Glen Rose Formation.

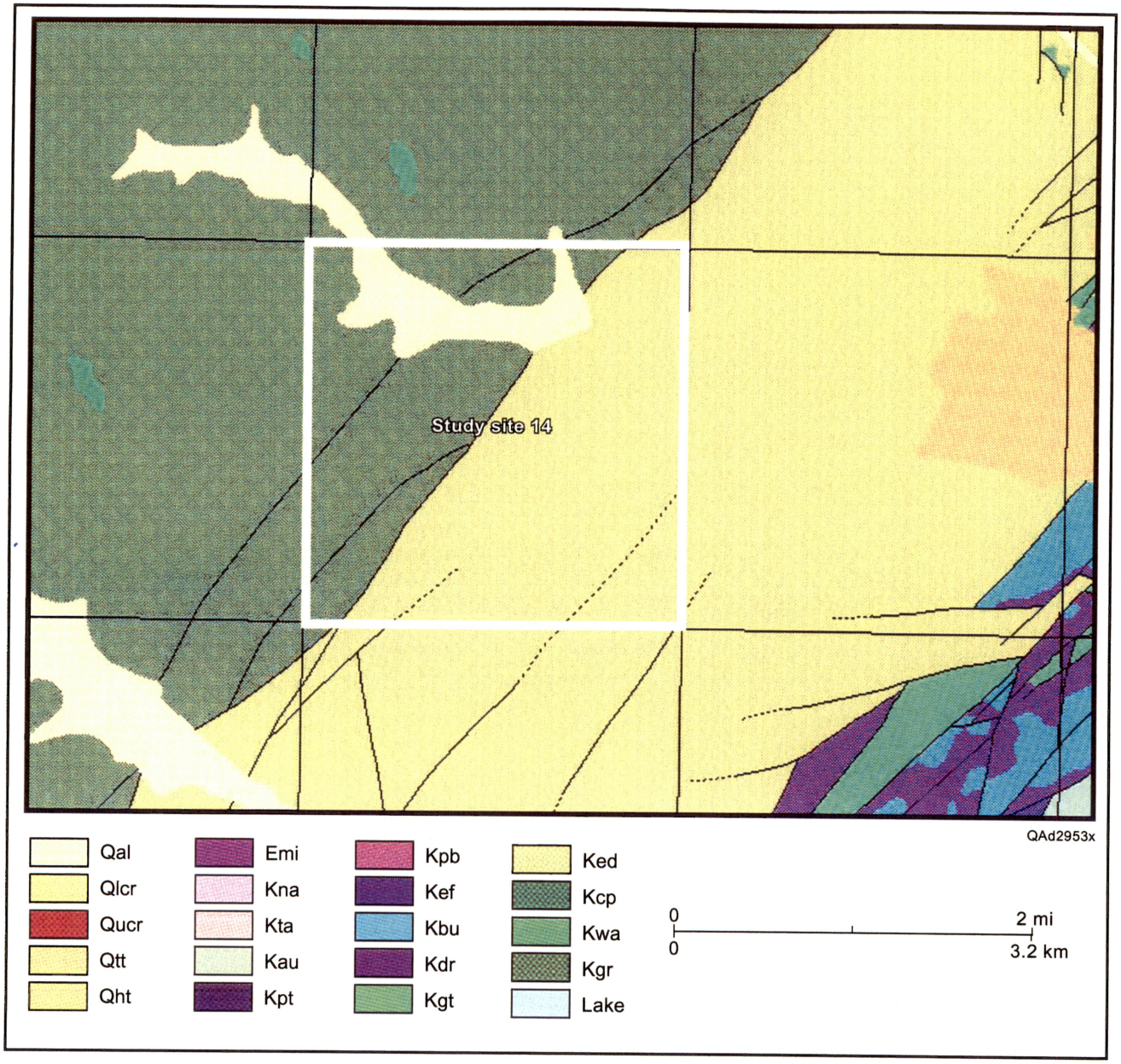

Figure 25. Geologic setting and location of study site 14 along major fault strands of the Balcones Fault Zone. Geology from digital geologic map data set (Tremblay and Andrews, 1997) constructed from *Geologic Map of the Austin, Texas, Area* (Garner and others, 1976). Tiles indicate areas of airborne lidar data.

Figure 26. Aerial photograph of study site 14. Suburban development has encroached on the hilly limestone terrain of the study site. Geologic setting shown in figure 25.

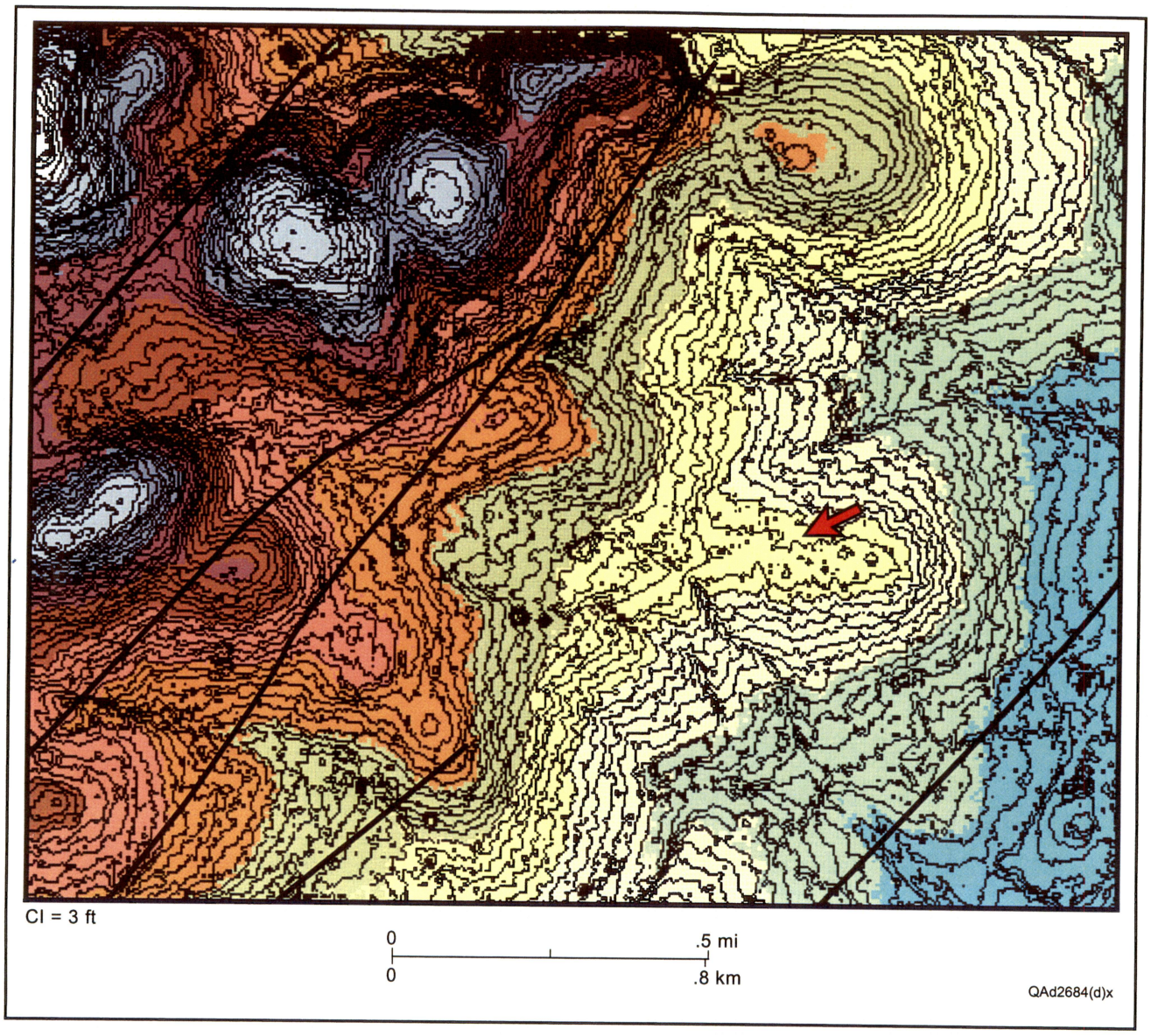

Figure 27. Faults and detailed topographic map constructed from lidar data at study site 14. Within hilly limestone terrain at this site, faults mapped by Garner and others (1976) cut through topographic lows between hill tops and flank hillsides. Arrow points across an area of subtle linear topography that aligns with a previously mapped fault. This linear topography may indicate fracture continuation through the limestone that was not recognized during previous mapping. Geologic setting shown in figure 25.